Transactions of the Royal Society of Edinburgh: Earth Sciences, **97**, 337–355, 2008 (for 2006)

Exploring the plutonic–volcanic link: a zircon U–Pb, Lu–Hf and O isotope study of paired volcanic and granitic units from southeastern Australia

A. I. S. Kemp, C. J. Hawkesworth, B. A. Paterson, G. L. Foster, P. D. Kinny, M. J. Whitehouse, R. Maas and EIMF

ABSTRACT: The relationship between plutonic and volcanic rocks is central to understanding the geochemical evolution of silicic magma systems, but it is clouded by ambiguities associated with unravelling the plutonic record. Here we report an integrated U–Pb, O and Lu–Hf isotope study of zircons from three putative granitic–volcanic rock pairs from the Lachlan Fold Belt, southeastern Australia, to explore the connection between the intrusive and extrusive realms. The data reveal contrasting petrogenetic scenarios for the S- and I-type pairs. The zircon Hf–O isotope systematics in an I-type dacite are very similar to those of their plutonic counterpart, supporting an essentially co-magmatic relationship between these units. The elevated $\delta^{18}O$ of zircons in these I-type rocks confirm a significant supracrustal source component. The S-type volcanic rocks are not the simple erupted equivalents of the granites, although the extrusive and plutonic units can be related by open-system magmatic evolution. Zircons in the S-type rocks define covariant ε_{Hf}–$\delta^{18}O$ arrays that attest to mixing or assimilation processes between two components, one being the Ordovician metasedimentary country rocks, the other either an I-type magma or a mantle-derived magma. The data are consistent with models involving incremental melt extraction from relatively juvenile magmas undergoing open-system differentiation at depth, followed by crystal-liquid mixing upon emplacement in shallow magma reservoirs, or upon eruption. The latter juxtaposes crystals with markedly different petrogenetic histories and determines whole-rock geochemical and textural properties. This scenario can explain the puzzling decoupling between the bulk rock isotope and geochemical compositions commonly observed for granite suites.

KEY WORDS: Hf isotope, Lachlan Fold Belt, O isotope, Silicic magma, zircon

The relationship between plutonic and volcanic rock bodies formed an integral part of the 'granite controversy' of the early twentieth century. Read (1948) asserted that these units originate in fundamentally different ways; plutons form by slow transformational processes in deep orogenic crust, whereas volcanic rocks have a shallow level, higher temperature origin. However, to N. L. Bowen, Read's main adversary, the volcanic units simply represent a more advanced stage of differentiation along a liquid line of descent compared to their plutonic counterparts (Bowen 1928). The implication is that the venting and eruption of variably fractionated magmas is intrinsic to the evolution of high-level granitic plutons. Numerous workers have since developed this theme (e.g. Langmuir 1989), and the link between intrusive and extrusive felsic rocks has thus become increasingly entwined. For example, recent studies infer that ignimbrites are 'erupted batholiths', formed by thermal rejuvenation of near-solidus granitic mushes (Bachmann *et al.* 2002; Bachmann & Bergantz 2004) or by the evacuation of long-lived, shallow-crustal magma chambers (Vasquez & Reid 2005), with the crystalline residues solidifying as plutons. Alternatively, Glazner *et al.* (2004) suggest that ignimbrite- and pluton-building processes are different; caldera-forming ignimbrite eruptions drain ephemeral melt-dominated reservoirs formed by rapid magmatic input, whereas pluton growth occurs in response to lower magmatic and thus thermal flux. An impediment to these models is that knowledge of the geochemical evolution of plutonic rocks lags behind that of volcanic systems, which have the advantage of preserving the melt composition and (potentially) primary liquidus mineralogy, and avoiding the textural and chemical equilibration that attends complete crystallisation. However, newly developed microanalytical techniques hold much promise for deciphering the plutonic archive (see also Davidson *et al.* 2007), enabling unparalleled scrutiny of the volcanic–plutonic link.

The Palaeozoic Lachlan Fold Belt (LFB) of southeastern Australia provides an intriguing perspective. The granites of this terrane are subdivided into two main groups, 'S-type', which have peraluminous minerals like cordierite and for which a supracrustal (metasedimentary) source is inferred, and the hornblende-bearing 'I-types' that are assigned infracrustal (meta-igneous) precursors (Chappell & White 1974). This distinction extends to felsic volcanic rocks. In some cases, the petrographic features and geochemistry of the crystal-rich volcanic units closely matches that of nearby granitic plutons (Chappell & White 1992), implying that the volcanic rocks are the erupted equivalents of the granites. This observation has been used to dismiss the importance of shallow-level fractional crystallisation processes, such that the granites might be cumulates and the volcanic units complementary fractionated liquids (Wyborn & Chappell 1986). It has also been argued that the phenocrysts preserve chemical equilibria established at near-source pressure and temperature (Wyborn *et al.* 1981; Wyborn & Chappell 1986), the latter being too low for the rocks to ever have been complete melts. These workers thus suggest that the entire phenocryst cargo, and by inference

many crystals in the associated granites, are restitic phases entrained from the source. This is at odds with the conventional magmatic interpretation of euhedral crystals in volcanic rocks (e.g. Vernon 1983), but has been cited as support for the restite-unmixing model (Chappell *et al.* 1987).

The main argument made above, that some complexes preserve directly equivalent plutonic and volcanic compositions, deserves closer scrutiny. Almost invariably, chemical compositions of the LFB volcanic rocks have been affected by alteration, obscuring original variations in K, Na and some trace elements on the whole-rock scale (Wyborn *et al.* 1981). Isotopic data are rarely available and may be similarly compromised by alteration. The claim of direct age equivalence is also dubious. Age constraints for the LFB volcanic rocks are largely based on field relations and litho-/bio-stratigraphy, and/or on K–Ar and Rb–Sr mineral ages for both volcanic and granitic units. These constraints are unlikely to allow anything other than broad age (within 5–10 Ma) comparisons. Where field relations unambiguously support a volcanic–granitic relationship, such as for the Late Devonian Violet Town Ignimbrite/Strathbogie Granite in central Victoria, the initial $^{87}Sr/^{86}Sr$ ratios for the erupted and intruded units are clearly different (Clemens 1989; Gray 1990). Detailed comparison of compositionally 'similar' volcanic and granitic rocks is thus not straightforward and is likely to be hampered by lack of reliable critical data.

The accessory phase zircon may hold the key to this issue. The chemical and isotopic information encoded within the growth zoning of this mineral provides a robust, alteration-resistant record of magmatic evolution, which can be retrieved by *in situ* microanalysis (Griffin *et al.* 2002; Kemp *et al.* 2005a; Belousova *et al.* 2006; Yang *et al.* 2006; Kemp *et al.* 2007). Zircon is amenable to U–Pb dating, allowing chemical or isotope variations to be placed into a chronological framework, and incorporates dual isotope tracers that both ascertain the crustal residence ancestry of the magma's source (e.g. Lu–Hf) and diagnose the input of supracrustal material by assimilation or mixing processes (e.g. $^{18}O/^{16}O$). The present authors report a comparative zircon U–Pb, O and Lu–Hf isotope study of zircon crystals from three putative plutonic–volcanic pairs of the LFB. The objectives are (1) to test the consanguinity or otherwise of the eruptive and intrusive rocks; (2) to constrain the magma sources; and (3) to unravel and compare the petrogenetic processes operating in the plutonic and volcanic realms.

1. Background

The LFB preserves the record of 100 Myrs of accretionary tectonic processes along the convergent east Gondwana continental margin (Gray & Foster 1997). Following the eastward retreat of the Ordovician Macquarie arc in the Early Silurian, voluminous silicic magmas intruded, or were erupted onto, a thick apron of quartz-rich turbidites that were largely craton-derived and accumulated on Cambrian oceanic crust. The major pulses of felsic magmatism in the eastern LFB occurred between 430 Ma and 390 Ma, resulting in elongate, meridionally trending batholiths aligned with the structural grain (Fig. 1). Younger (370–360 Ma) magmatism further west in central Victoria involved the emplacement of isolated post-compressional plutons associated, in some cases, with large ignimbrite deposits preserved in cauldron complexes (Fig. 2). The LFB silicic magmas were generated at mid-crustal depths (<30 km), but the exposed metasedimentary sequence only locally exceeds greenschist facies in thrust-bound metamorphic complexes. Together with the preservation of the ignimbrites,

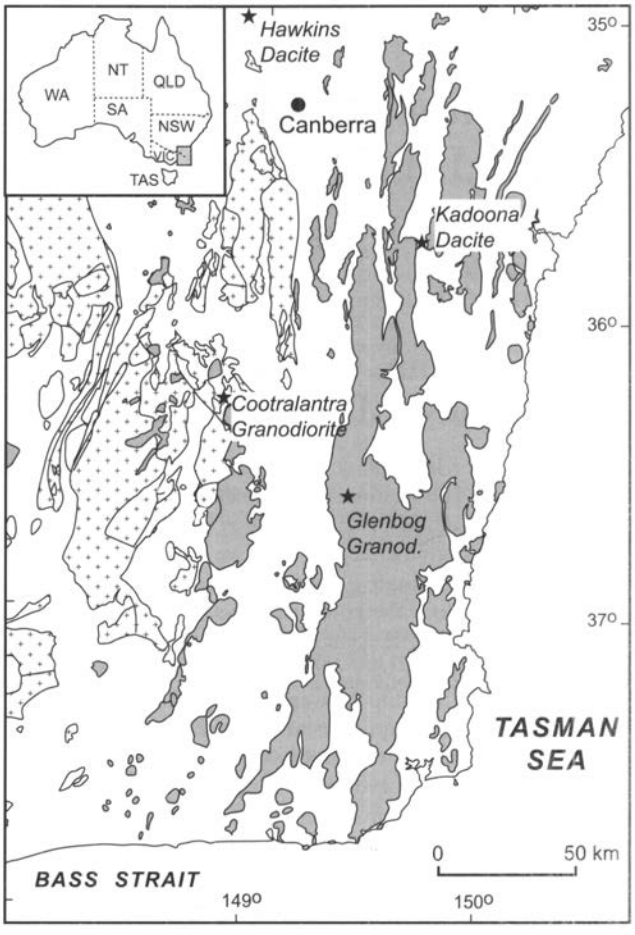

Figure 1 Simplified geological map of the eastern Lachlan Fold Belt showing the location of the granitic and volcanic samples referred to in the text (stars). S-type granites are shown with cross symbols, whereas I-type granites, A-type granites and gabbros are shaded.

this demonstrates that regional post-orogenic uplift in the LFB was relatively minor.

Silicic igneous rocks of the LFB are compositionally diverse and have been grouped into suites and supersuites on the basis of shared and distinctive petrographic or geochemical features. Each suite exhibits coherent, typically linear variation for element–element pairs and is believed to correspond to a specific source rock composition (Chappell *et al.* 1987). This diversity extends to isotope data. Sr–Nd–O isotope ratios for the I- and S-type granitic suites define distinct trends, but there is also considerable overlap (Fig. 3). The origin of these isotope variations has received much attention. McCulloch & Chappell (1982) attribute the Sr–Nd isotopic dispersion in I-type granites to derivation from mafic underplates of different mantle-extraction age, whereas the isotope variation in the S-types is thought to reflect the chemical maturity of the metasedimentary sources. However, metasedimentary protoliths with the appropriate isotope (or chemical) composition to produce most of the LFB S-type granites have yet to be identified (Fig. 3). Other workers assign the transitional I–S-type isotope arrays to mixing between magmas sourced from the Ordovician metasedimentary basement and either one (Gray 1984, 1990) or two (Collins 1996; Keay *et al.* 1997) isotopically primitive end-members. These hypotheses have markedly different implications for Palaeozoic circum-Pacific crustal evolution (e.g. Collins 1998; Kemp *et al.* 2007). Paradoxically, however, mixing models based on isotopes are difficult to reconcile with the observed geochemical variation of granite suites (McCulloch & Chappell 1982). Either the mixing models are invalid, or the processes that control bulk

https://doi.org/10.1017/S0263593300001498 Published online by Cambridge University Press

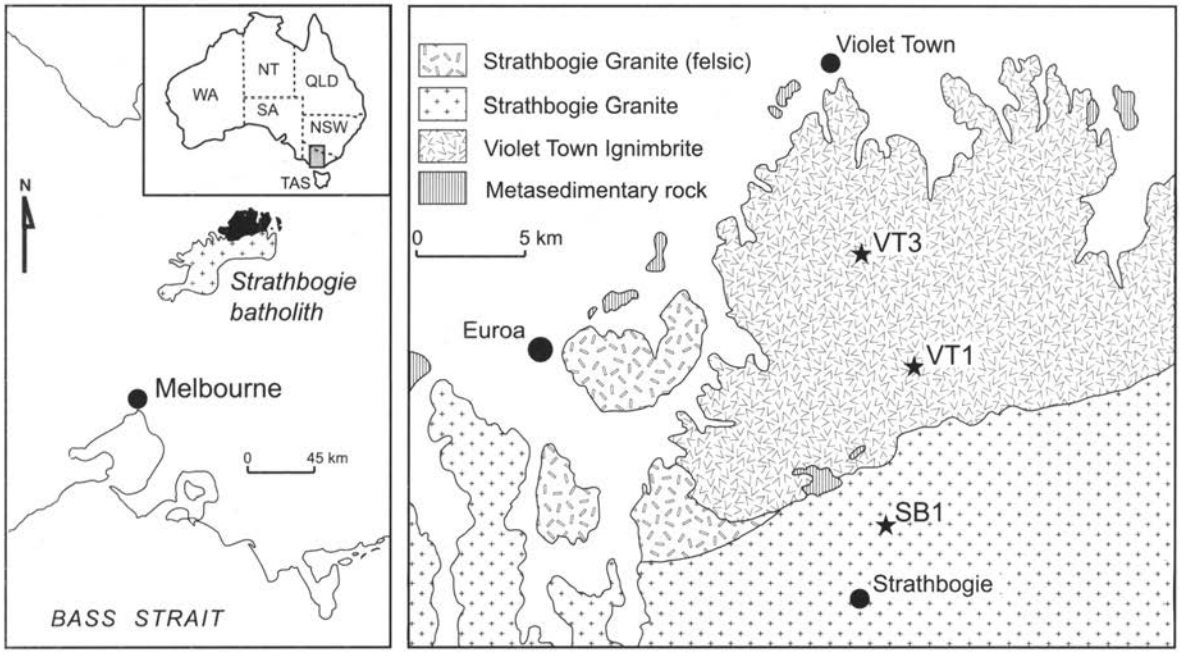

Figure 2 Location of the Violet Town Ignimbrite and Strathbogie Batholith in central Victoria showing the sample localities of the rocks examined by this study (stars) (modified after Chappell *et al.* 1991 and Elburg 1996).

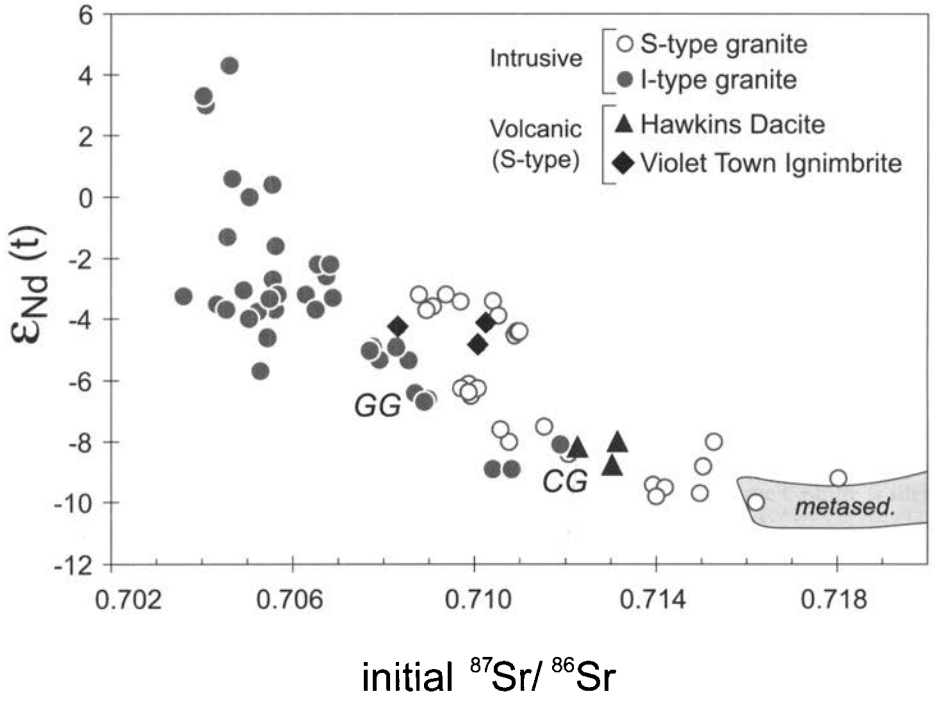

Figure 3 Whole-rock Sr and Nd isotope composition of S- and I-type granites of the Lachlan Fold Belt, computed at their crystallisation age (CG) Cootralantra Granodiorite; (GG) Glenbog Granodiorite) and compared to the Sr–Nd isotope field of the exposed LFB metasedimentary rocks (shaded). Note the contrasting isotope compositions of two S-type volcanic units. Data sources include: McCulloch & Chappell 1982; Chappell *et al.* 1991; McCulloch & Woodhead 1993; Elburg 1996; Waight & Maas unpublished data.

rock geochemistry were different from those causing the isotope variations; this is explored further below.

2. Sample details

Three chemically analogous volcano–plutonic associations have been targeted, the Kadoona Dacite–Glenbog Granodiorite (I-type), the Hawkins Dacite–Cootralantra Granodiorite (S-type) and the Violet Town Ignimbrite–Strathbogie Granite (S-type). Table 1 summarises the salient features of these units, and Table 2 lists the geochemistry of each sample.

2.1. Kadoona Dacite–Glenbog Granodiorite (I-type)

The I-type Kadoona Dacite (Wyborn & Chappell 1986) is an ignimbrite unit of 40 km strike length that outcrops near the northern extremity of the Glenbog Suite. At its type locality, it is a massive brownish grey, strikingly crystal-rich rock containing abundant plagioclase (An_{48-55}), strongly embayed quartz,

https://doi.org/10.1017/S0263593300001498 Published online by Cambridge University Press

Table 1 A summary of the rock samples from which zircons were analysed in this study. Minerals listed for the volcanic rocks represent the phenocryst assemblage (percent crystals is shown in parentheses). Data sources as for Figure 3 (n/a=not available)

Unit/sample	Type	Age (Myr)	Major mineralogy	$^{87}Sr/^{86}Sr$ (t)	ε_{Nd} (t)
Kadoona Dacite (KDD)	I	414 ± 5	q-pl-bi-cpx-opx (60%)	n/a	n/a
Glenbog Granodiorite (GB1)	I	414 ± 5	q-pl-kfs-hbl-bi	0·70879	−6·4
Hawkins Dacite (HV1)	S	430 ± 4	q-pl-bi-opx-crd-gt (60%)	0·71317	−8·0
Cootralantra Granodiorite (BB1)	S	430 ± 5	q-pl-kfs-bi-crd	0·71206	−8·4
Violet Town Ignimbrite (VT3)	S	373 ± 3	q-pl-kfs-bi-opx-crd-gt (55%)	0·70832 to 0·71109	−4·2 to −4·8
Violet Town Ignimbrite (VT1)	S	373 ± 3	q-pl-kfs-bi-opx-gt-crd (50%)		
Strathbogie Granite (SB1)	S	366 ± 3	q-pl-kfs-bi-crd-gt	0·71154	n/a

Table 2 The whole-rock geochemistry of the targeted volcanic–plutonic rock units (A.S.I., alumina saturation index, molar $Al_2O_3/[CaO+Na_2O+K_2O]$). Data for BV5 and AB6 are from Chappell & White (1992), and data for SV51 are from Chappell *et al.* (1993) for samples collected from the same outcrop as the rocks analysed in this study. The geochemical data for BV5, AB6 and SV51 were determined by X-ray fluorescence (XRF), whereas for BB1, VT3 and SB1 the major and some trace elements (Sc, V, Cr, Ni, Cu and Zn) were measured by XRF, and the other trace elements by solution ICP–MS. The quoted number of decimal places reflects analytical precision

Rock Unit	Kadoona Dacite	Glenbog Granodiorite	Hawkins Dacite	Cootralantra Granodiorite	Violet Town Rhyodacite	Strathbogie Granite
Sample no.	BV5	AB6	SV51	BB1	VT3	SB1
SiO_2	66·17	67·39	68·05	66·56	68·20	70·81
TiO_2	0·59	0·53	0·61	0·62	0·68	0·47
Al_2O_3	14·52	14·48	14·41	14·79	15·24	14·05
Fe_2O_3	1·80	1·58	1·15	1·01	1·31	0·11
FeO	3·40	3·02	3·31	4·17	2·95	2·99
MnO	0·09	0·09	0·06	0·08	0·07	0·06
MgO	2·14	1·72	2·05	2·38	1·48	0·99
CaO	4·72	4·32	2·68	3·43	2·92	1·51
Na_2O	2·46	2·63	2·03	1·88	2·55	2·47
K_2O	2·74	2·99	3·58	3·15	3·53	4·49
P_2O_5	0·11	0·11	0·15	0·14	0·19	0·17
LOI	1·15	1·16	1·60	1·55	0·45	1·48
Total	100·10	100·17	99·87	99·94	99·85	99·82
ASI	0·95	0·96	1·23	1·16	1·14	1·21
Sc	21	20	15	18	10	8
V	106	101	93	116	74	47
Cr	17	9	57	58	37	28
Ni	5	4	22	17	17	14
Cu	9	3	14	14	19	13
Zn	60	55	73	74	73	70
Nb	9	9	10·5	11·8	15·6	13·6
Y	29	32	32	31·9	42·3	34·9
Zr	162	145	189	172·8	235·7	180·6
Ga	16·6	15·8	18·2	18·5	20	18·9
Rb	124	135	170	167·2	165·8	247·9
Sr	168	148	138	151·8	186·4	97·8
Ba	440	415	530	453	1015	753
La	26	26	22	33·0	42·7	32·9
Ce	61	62	74	66·8	87·4	67·7
Nd				30·9	41·3	32·2
Pb	26	15	25	21·2	20·5	21·3
Th	16	16	20	15·6	16·3	16·6
U	3	3	4	3·5	3·5	7·6

augite and orthopyroxene phenocrysts in a devitrified groundmass mosaic with a barely discernible eutaxitic fabric. Zircons are sparsely scattered through the groundmass, and form rare inclusions in plagioclase and pyroxene crystals. Zircon inclusions also occur in phenocrysts of the other volcanic rocks examined herein. A variety of exchange thermometers establish pre-eruption temperatures of 850–950°C for the Kadoona Dacite, whereas a clinopyroxene–plagioclase–quartz equilibration pressure of 720 MPa is estimated (Wyborn & Chappell 1986). The Glenbog Granodiorite of the Glenbog Suite outcrops along the eastern edge of the Bega Batholith south of the Kadoona Dacite. It is a medium to coarse-grained mesocratic rock with large quartz crystals, cream plagioclase and abundant hornblende prisms, with interstitial to poikilitic

orthoclase. Some hornblende grains enclose clinopyroxene relicts.

The Kadoona Dacite and lower silica Glenbog Suite plutons have very similar bulk rock geochemistry (Wyborn & Chappell 1986), being unified in particular by Na and Sr concentrations that are much lower than other LFB I-types and metaluminous intrusives of the American Cordillera. For this reason, the Kadoona Dacite and Glenbog Granodiorite are regarded as the type example of a consanguineous I-type volcano–plutonic association (Wyborn & Chappell 1986; Chappell *et al.* 1987). Nevertheless, there are some chemical differences between these units. The Kadoona Dacite has a relatively restricted compositional range, on average having lower SiO_2 (64–67% compared to 65·5–74% SiO_2 for the Glenbog plutons) and extending to distinctly higher MgO, CaO and Sr than the lower silica extrapolation of the Glenbog Suite chemical trends (Wyborn & Chappell 1986). These differences are evident between the specific samples of this study (Table 2) and have been attributed to derivation of these units from subtly different protoliths (Wyborn & Chappell 1986). However, they might equally reflect phenocryst accumulation in the dacite or the input of more juvenile material into the volcanic system; the legacy of the latter is potentially preserved by the Hf–O isotope compositions of crystallising zircons. Bulk rock isotope data are not available for the Kadoona Dacite, however the Glenbog Granodiorite has amongst the most crust-like isotope compositions (i.e. elevated $^{87}Sr/^{86}Sr$ and $\delta^{18}O$, low ε_{Nd}) of I-type granites in eastern Australia (Table 1, Fig. 3).

2.2. Hawkins Dacite–Cootralantra Granodiorite (S-type)

Volcanic units of the Silurian S-type Hawkins Suite form a belt extending from Canberra northwest towards the township of Cowra. They are included as part of the Bullenbalong Supersuite, lower silica members of which include cordierite-rich tonalites and granodiorites replete with metasedimentary enclaves. The Hawkins Dacite sample of this study was collected from the type outcrop of Chappell *et al.* (1993). It resembles the Kadoona Dacite, containing 60% phenocrysts dispersed through a finely recrystallised felsic matrix, but is distinguished by the occurrence of cordierite ± almandine and the absence of calcic pyroxene (Table 1). Mg partitioning between co-existing garnet and cordierite yield P = 500–600 MPa and T = 800 °C, believed to correspond to anatectic conditions in the source region (Wyborn *et al.* 1981). Zircons occur as isolated crystals in the groundmass and typically smaller inclusions in all phenocrysts except garnet. They are especially prominent in cordierite, both where this mineral forms euhedral–subhedral phenocrysts and where it occurs as symplectites with orthopyroxene around garnet. Chappell *et al.* (1993) highlighted the geochemical similarity between the Hawkins Dacite and the Cowra Granodiorite, which intrudes correlatives of the volcanics in the northern part of the belt. However, the Cowra Granodiorite appears to be 10–15 Myr younger than the Hawkins Dacite, and other workers have noted differences in initial Sr and Nd isotope compositions between the dacite and the Cowra Granodiorite (Waight *et al.* 2001). The present authors have instead chosen to compare the Hawkins Dacite with the Cootralantra Granodiorite of the Berridale Batholith further south, following Wyborn *et al.* (1981). Although these units are some distance apart they are coeval (see below) and have similar geochemical (Wyborn *et al.* 1981) and Sr–Nd isotope compositions (Table 1). The Cootralantra Granodiorite sample of this study is a medium grained equigranular rock with a foliation of aligned biotite plates and plagioclase prisms. Abundant cordierite is invariably replaced by sheaves of mica. The whole-rock $\delta^{18}O$ of a sample from this pluton is 10·3‰ (O'Neil & Chappell 1977).

2.3. Violet Town Ignimbrite–Strathbogie Granite (S-type)

The Violet Town Ignimbrite crops out in central Victoria, north of Melbourne (Fig. 2). It comprises a 430 m thick rhyodacite and rhyolite sequence that is intruded and metamorphosed near its base by the subvolcanic Strathbogie batholith, which shows evidence of pressure quenching and high-level crystallisation (Phillips *et al.* 1981). The petrology of the ignimbrite is documented by Clemens & Wall (1984) and Elburg (1996). The former calculate average equilibration conditions for early phenocryst assemblages of 850 °C and 350 MPa, but infer that the bulk of crystallisation and thus magmatic evolution proceeded in a high level magma chamber from a water-undersaturated parental rhyodacite magma. Two ignimbrite samples were collected. VT1 is a rhyodacite from near the base of the sequence that contains variably fragmented phenocrysts (50%) of quartz, plagioclase, orthoclase (minor), biotite, orthopyroxene, cordierite and subordinate garnet (with decompression coronas of cordierite and orthopyroxene) in a microcrystalline felsic groundmass. All mafic phases contain zircon inclusions. Aligned biotite phenocrysts, pumice fragments and lithic inclusions define an ash-flow compaction fabric. VT3 is a similar-looking rhyodacite from the mid- to upper part of the volcanic pile that has relatively abundant garnet phenocrysts and a marginally coarser groundmass. The Violet Town Ignimbrite samples have variable Sr–Nd isotope compositions (Fig. 3) and $\delta^{18}O$ (10·4–11·7‰).

The sample from the Strathbogie batholith was collected near its northern contact with the ignimbrite. It comprises coarse crystals of quartz, tabular K-feldspar (to 1 cm) and plagioclase, large reddish-brown biotite plates, conspicuous pale blue cordierite prisms (to 20 mm across), and uncommon garnet. This granite is compositionally more evolved than the rhyodacites (Table 2), although the Strathbogie Granite and Violet Town Ignimbrite define rather similar trends on geochemical variation diagrams. Together with the close spatial relationship and petrographic similarity, this suggests a genetic link between these rock bodies. However, the initial $^{87}Sr/^{86}Sr$ of the Strathbogie Granite is slightly more radiogenic (Table 1).

3. Methods and results

Zircons from all samples were subjected to the same micro-analytical techniques described by Kemp *et al.* (2006). The analytical strategy was to acquire and compare data from the same *general* growth phase of each zircon crystal. Following cathodoluminescence and back-scattered electron imaging, zircons were first dated by ion microprobe using the SHRIMP II at Curtin University, Perth, or a Cameca ims 1270 at the Swedish Museum of Natural History, Stockholm. Selected grains were then analysed for major and minor elements using a Cameca SX-100 electron microprobe at the University of Bristol, so that any intra-grain isotope variation could be placed into a chemical context. The O isotope analysis was conducted by ion microprobe at the University of Edinburgh, and values are reported relative to bracketing analyses of primary standard zircon 91500 to correct for instrumental mass bias and drift. The variation in two secondary standard zircons measured during the same period was between 0·2–0·3‰ at one standard deviation (s.d.). Lastly, the Hf isotope composition of the same part of each crystal was determined

Table 3 Details of standard zircon Hf isotope data acquired for each session in which zircons of the different samples were analysed ($^{176}Hf/^{177}Hf$ values are corrected to JMC 475=0·28216). The solution ICP–MS $^{176}Hf/^{177}Hf$ values of separated Hf fractions from these standard zircons are: 0·282686 ± 8 for Temora, 0·282306 ± 8 for 91500 and 0·282507 ± 6 for Mud Tank (from Woodhead & Hergt 2005, errors quoted at 2 standard deviations)

Session date	Samples analysed	Standards analysed	Laser ablation $^{176}Hf/^{177}Hf$	2 s.d. (ε units)
16 Aug 04	KDD, GB1	Temora 2	0·282685 ± 22, n=7	0·78
		91500	0·282306 ± 9, n=1	
28 Nov 04	HV1, VT1, VT3	Temora 2	0·282691 ± 18, n=7	0·64
		91500	0·282304 ± 8, n=3	0·28
		Mud Tank	0·282500 ± 28, n=2	0·99
29 Nov 04	BB1	Temora 2	0·282676 ± 6, n=5	0·21
		Mud Tank	0·282486 ± 6, n=2	0·21
30 Nov 04	SB1, VT3	Temora 2	0·282683 ± 14, n=11	0·50
		91500	0·282290 ± 4, n=2	0·14
		Mud Tank	0·282495 ± 18, n=9	0·64
02 May 05	KDD, GB1	Temora 2	0·282679 ± 18, n=11	0·64
		91500	0·282304 ± 28, n=7	0·99
		Mud Tank	0·282491 ± 18, n=2	0·64
27 Feb 07	GB1	Temora 2	0·282690 ± 24, n=17	0·85
		91500	0·282308 ± 28, n=4	0·99
		Mud Tank	0·282498 ± 8, n=2	0·28
28 Feb 07	KDD, GB1	Temora 2	0·282688 ± 20, n=20	0·85
		91500	0·282308 ± 2, n=2	0·07
		Mud Tank	0·282506 ± 16, n=8	0·57
29 Feb 07	HV1	Temora 2	0·282689 ± 18, n=26	0·64
		Mud Tank	0·282508 ± 12, n=4	0·42

by laser ablation multi-collector ICP-MS at the University of Bristol, targeting (where possible) the pits generated by the foregoing ion microprobe analysis. Spot sizes of 40–50 μm were utilised, excavating pits between 20–30 μm deep. As a monitor of data quality, analyses of homogeneous standard zircons were regularly interspersed with sample zircons throughout each analytical session (Table 3). The $^{176}Hf/^{177}Hf$ ratio of standards in all sessions are reproducible at the <1 ε_{Hf} (2 s.d.) unit level; any variation in the sample zircons significantly outside of this is likely to be of geological origin.

3.1. U–Pb data

The U–Pb isotope results are summarised by Figure 4. Zircons in the I-type Kadoona Dacite and Glenbog Granodiorite are elongate and dominated by [100] prisms, with variable development of [101] and [211] terminations (Fig. 5). The weighted mean $^{206}Pb/^{238}U$ age of zircons in the Kadoona dacite is 414 ± 5 Ma (n=16, rejecting one point), which is identical to the age of melt-precipitated zircon within an igneous-textured enclave contained by the Glenbog Granodiorite (Chen & Williams 1990). We infer this enclave to have solidified at the same time as the host granodiorite, and on this basis, conclude that the zircon crystallisation age of the Kadoona Dacite and Glenbog Granodiorite are indistinguishable. Some of the Kadoona Dacite zircons have rounded to slightly embayed cores, one of which yielded a pre-magmatic U–Pb age (1050 Ma), confirming an inherited origin. No further attempt was made to characterise the ages of these cores. Inherited zircon cores also occur in the Glenbog Granodiorite, as well as in other LFB I-type granites (Williams 1992; Kemp *et al.* 2005a).

In contrast to the I-type Kadoona Dacite/Glenbog Granodiorite pair, inherited cores are abundant in zircons of the S-type Hawkins Dacite and Cootralantra Granodiorite. The zircon morphology in both samples is essentially controlled by the shape and size of these inherited cores; stubby crystals with large [211] pyramids are most common. Determining a reliable age from the generally thin (<50 μm) magmatic zircon rims poses a challenge even for ion microprobe analysis. Nevertheless, magmatic zircon ages from the Hawkins Dacite and Cootralantra Granodiorite zircons cluster around 430 Ma (Fig. 4), indicating essentially coeval crystallisation. Magmatic zircons of both samples show the same large range of U contents (100–800 ppm) and rather low average Th/U ratios (0·25) (Figs 6, 7). Older cores in both samples show a spread of ages from 450 Ma to 2700 Ma, with major peaks at 500–600 and 1000–1200 Ma, typical of many LFB S-type granites and ubiquitous in East-Gondwana margin detrital zircon populations (e.g. Ireland *et al.* 1998; Kemp *et al.* 2006).

Age inheritance is much less common in zircons of the S-type Violet Town Ignimbrite and Strathbogie Granite (Fig. 4). Rhyodacite zircons are predominantly elongate to acicular in shape, with typical magmatic zoning including oscillatory and sector zoning, and complex trace element profiles (Fig. 8). Grains with lower aspect ratios may contain corroded inherited cores that are smaller than those of the Hawkins Dacite–Cootralantra Granodiorite zircons and surrounded by thick oscillatory-zoned magmatic overgrowths. The Strathbogie Granite zircons have very similar morphology and zoning characteristics. Some elongate grains in the rhyodacite and granite samples show irregular or convolute zone boundaries that resemble resorption surfaces. The ignimbrite-hosted zircons yield a pooled weighted average $^{206}Pb/^{238}U$ age of 373 ± 3 Ma (Fig. 4), identical to the Rb–Sr age quoted by Clemens & Wall (1984). Field relationships permit the Strathbogie Granite to be younger, and this is borne out by the zircon Pb/U age of 366 ± 3 Ma, although the two ages almost overlap within error. Bierlein *et al.* (2001) report a SHRIMP $^{206}Pb/^{238}U$ zircon age of 374 ± 2 Ma for another sample of Strathbogie Granite, suggesting essentially coeval emplacement of the ignimbrite and granite (the pooled $^{206}Pb/^{238}U$ age of all magmatic zircon analyses quoted by Bierlein *et al.* 2001 is 366 ± 6 Ma). On average, the Th/U ratios of the Violet

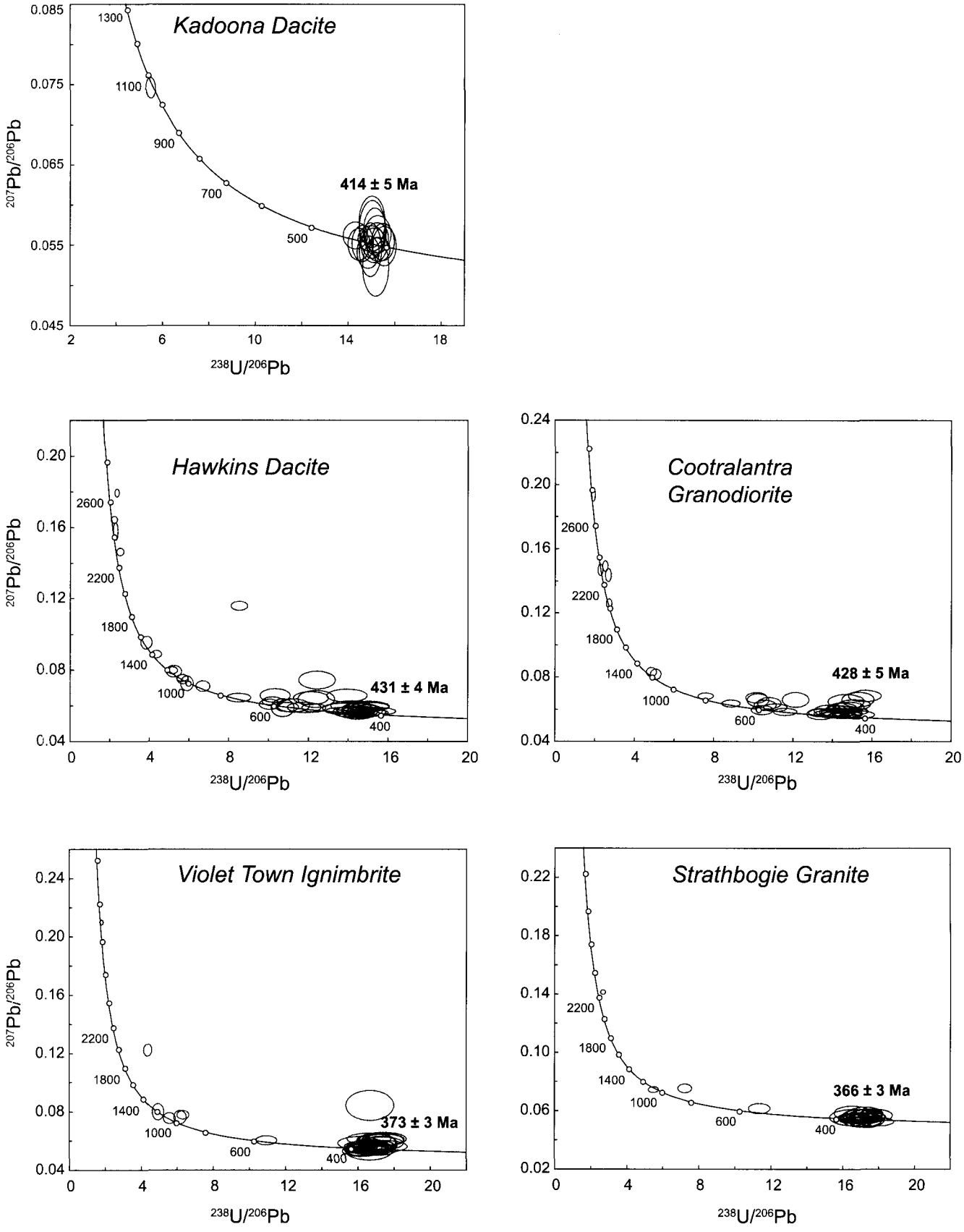

Figure 4 Terra-Wasserburg U–Pb isotope concordia diagrams for zircons of the Kadoona Dacite (I-type), Hawkins Dacite–Cootralantra Granodiorite (S-type) and Violet Town Ignimbrite–Strathbogie Granite (S-type), as measured by ion microprobe (error ellipses are plotted at 1 σ). The weighted average, common lead corrected $^{206}Pb/^{238}U$ ages are indicated for each unit.

Town-Strathbogie samples (0·5–0·6) are higher than those of the Hawkins–Cootralantra zircons (Fig. 7). The Strathbogie Granite zircons extend to markedly higher U content and thus lower Th/U than zircons of the Violet Town Ignimbrite, presumably reflecting the greater degree of differentiation of the host magma.

https://doi.org/10.1017/S0263593300001498 Published online by Cambridge University Press

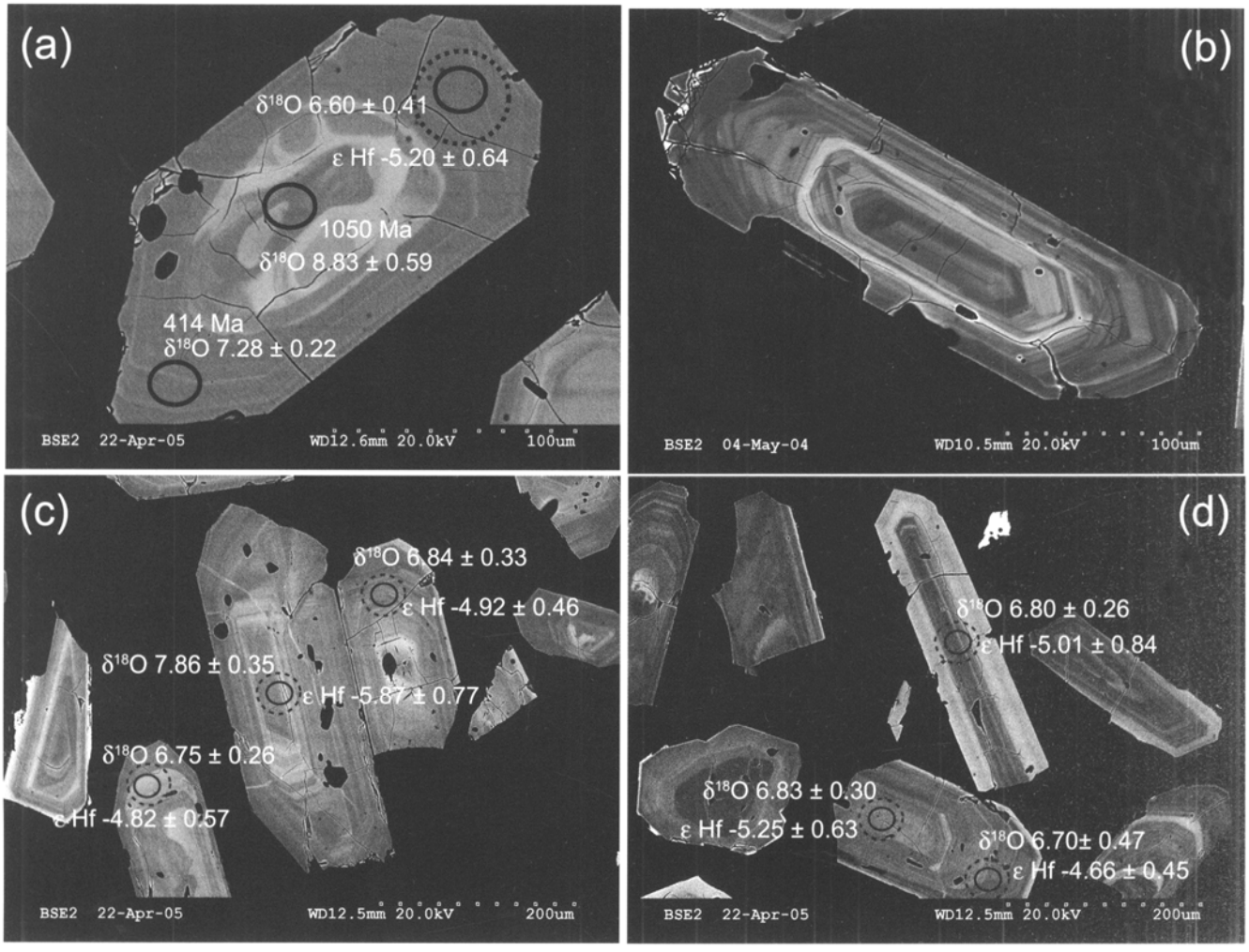

Figure 5 Back-scattered electron images showing the morphology, ages and O and Hf isotope characteristics of selected zircons in the Kadoona Dacite (a and b) and Glenbog Granodiorite (c and d). The approximate sizes of the O and Hf isotope pits are indicated. Image (a) shows an inherited zircon core in the Kadoona Dacite. The $\delta^{18}O$ notation represents the per mil deviation of the measured $^{18}O/^{16}O$ ratio relative to that of standard mean ocean water, VSMOW.

3.2. O isotopes

In situ oxygen isotope data for zircons of the three volcanic-granite pairs are shown in Figure 9. Oxygen isotope compositions in zircon, like those in other igneous minerals, depend on $\delta^{18}O$ of the parent melt and on the $^{18}O/^{16}O$ partitioning between melt and the growing zircon. Melt-zircon isotopic fractionation varies with melt composition and follows a linear relationship with SiO_2 content, whereby $\Delta^{18}O$ (Zrc–WR) ranges from $-0{\cdot}5$‰ for mafic melts to -2‰ for silicic derivatives (Valley 2003; Valley *et al.* 2005). This implies that a zircon with $\delta^{18}O$ of 5‰ could be in equilibrium with a basaltic magma having $\delta^{18}O = 5{\cdot}5$‰, or with a rhyolitic magma with $\delta^{18}O = 6{\cdot}5$–7‰. The $\delta^{18}O$ (zircon) value is thus not readily changed by closed system differentiation, but it is sensitive to open-system mixing or assimilation processes that change the $\delta^{18}O$ of the bulk magma (Valley *et al.* 2005).

The $\delta^{18}O$ values of zircons in the Kadoona Dacite fall between 6·3‰ and 7·9‰, with an average of $7{\cdot}2 \pm 0{\cdot}3$‰ (n = 38, 1 s.d.). This $\delta^{18}O$ range slightly exceeds that shown by homogeneous zircon standards (Fig. 9). Inherited cores have similar $\delta^{18}O$, except for one core with $\delta^{18}O$ close to 9‰ (Fig. 5). Magmatic zircons in the Glenbog Granodiorite also show limited inter- and intra-grain O isotope variability (Fig. 5). The $\delta^{18}O$ values are clustered between 6·4‰ and 7·3‰, but the average $\delta^{18}O$ of the entire population ($6{\cdot}9 \pm 0{\cdot}3$‰, n = 46) is lower that of the Kadoona Dacite zircons. This $\delta^{18}O$ offset is probably significant, although the range of $\delta^{18}O$ in the volcanic and plutonic zircons overlaps within analytical error. Two zircons in the Glenbog Granodiorite have $\delta^{18}O$ values approaching 7·9‰, distinctly higher than in any of the other analytical sites for the granodiorite zircons.

Examination of intra-crystal O–Hf isotope variation in the magmatic part of zircons from the Hawkins Dacite and Cootralantra Granodiorite was more difficult, due to the thin melt-precipitated rims of these grains. Measured $\delta^{18}O$ in the Hawkins Dacite zircon rims vary from 8–10‰ (average $9{\cdot}1 \pm 0{\cdot}5$‰ 1 s.d.), about twice the range shown by the zircon standards. One wholly melt-precipitated zircon shows no detectable $\delta^{18}O$ difference between core and rim, despite variations in trace element contents and Hf isotope compositions (Fig. 6). Magmatic zircons of the Cootralantra Granodiorite also show a 2‰ range in $\delta^{18}O$ without discernable within-grain variation, but the average $\delta^{18}O$ is lower than in the Hawkins Dacite zircons (average $8{\cdot}4 \pm 0{\cdot}6$‰, 1 s.d.). Zircon $\delta^{18}O$ in both samples is consistent with derivation from a parent magma with $\delta^{18}O$ of 10–11‰, which is compatible with the inferred metasedimentary source rocks. Contrasts in $\delta^{18}O$ of up to 6·6‰ between inherited cores and magmatic overgrowths in zircons of both rocks reflect the sluggish diffusion of O in zircon under magmatic conditions (Peck *et al.* 2003).

https://doi.org/10.1017/S0263593300001498 Published online by Cambridge University Press

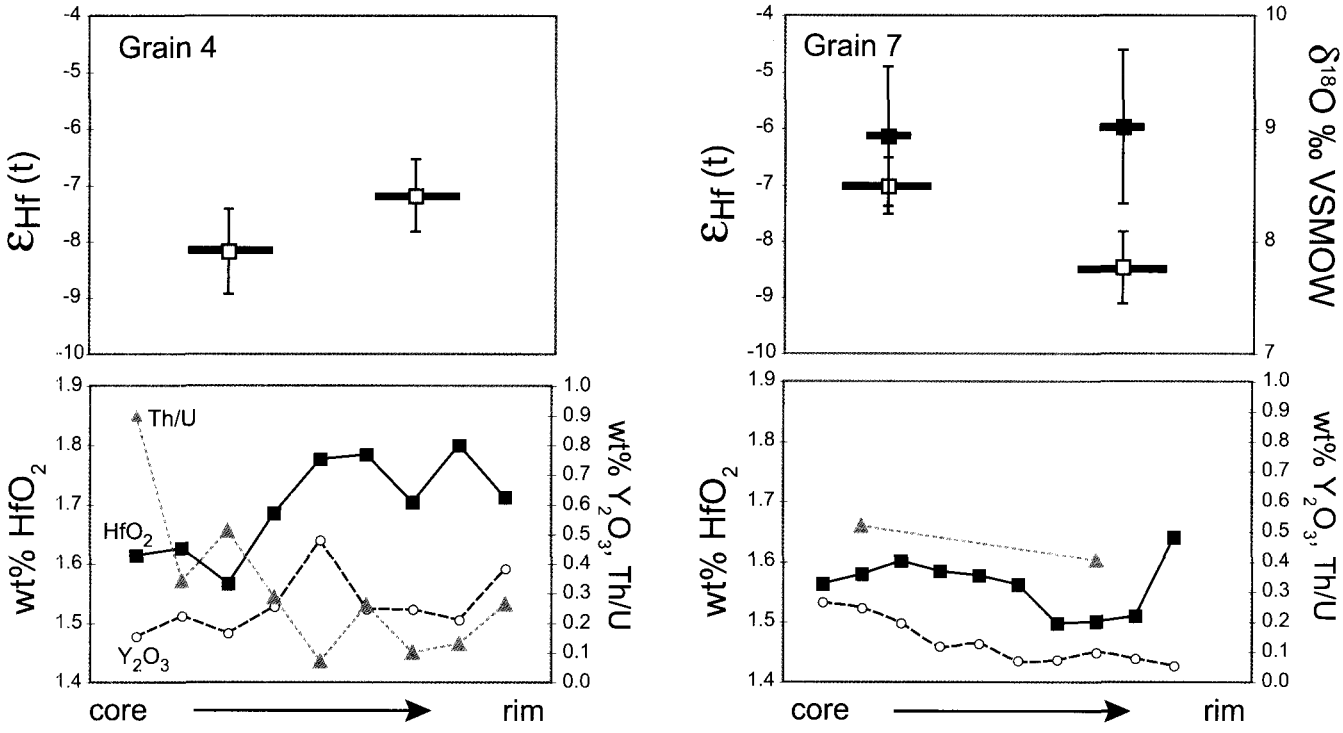

Figure 6 Trace element and Hf–O isotope characteristics of two magmatic zircons in the Hawkins Dacite. The bottom panel shows core-rim electron microprobe traverses for HfO_2, Y_2O_3 and Th/U (Th contents were mostly below detection for grain 7), whereas the top panel shows the Hf (open symbols) and O (closed symbols) isotope composition determined for the same part of each crystal; the horizontal bar depicts the spatial resolution of the isotope analyses in relation to the electron probe traverse. Error bars are shown at 2 s.e.

Zircon $\delta^{18}O$ in the S-type Violet Town Ignimbrite samples varies from 7·5‰ to 9·9‰, with zircons in VT1 having slightly lower average $\delta^{18}O$ (8·2 ± 0·8 at 1 s.d., compared to 8·6 ± 0·6‰ for VT3). Most ignimbrite zircons would therefore crystallise from magmas of average $\delta^{18}O$ around 9–10·5‰, which is lower than the whole-rock values reported by Elburg (1996). The whole-rock $\delta^{18}O$ may have been elevated by alteration, or, alternatively, the specific ignimbrite samples analysed by Elburg (1996) may be slightly accumulative with respect to ^{18}O-enriched minerals like quartz or feldspar. Traverses across magmatic zircons in both Violet Town Ignimbrite samples revealed abrupt fluctuations in trace element contents but no significant oxygen (or Hf) isotope heterogeneity (Fig. 8). These trace element profiles therefore attest to complex crystallisation histories. The Strathbogie Granite zircons are ^{18}O enriched compared to the ignimbrite-hosted zircons and exhibit the largest range in $\delta^{18}O$ (average 9·8 ± 1·2‰). Most zircon grains have $\delta^{18}O$ between 8‰ and 10·5‰, but analyses of one sector-zoned crystal yielded $\delta^{18}O$ of 12·5‰ and 12·7‰.

3.3. Lu–Hf isotopes

Figure 10 summarises the Hf isotope data obtained from zircons of the three suites. The I-type Kadoona Dacite zircons show a spread of less than 2 ε_{Hf} units (average ε_{Hf} − 5·2 ± 0·4, 1 s.d.) and a modest range of $^{176}Lu/^{177}Hf$ ratios. There is no obvious correlation between ε_{Hf} and $\delta^{18}O$ for the same crystal (Fig. 11). The Glenbog Granodiorite zircons have very similar ε_{Hf} (average − 5·0 ± 0·5, 1 s.d.) and $^{176}Lu/^{177}Hf$. The uniform zircon Hf isotope signatures argue against significant shifts in the magmatic $^{176}Hf/^{177}Hf$ ratio during zircon crystallisation in these I-type magmas.

As is the case for oxygen isotopes, zircons of the S-type rocks studied here show greater Hf isotopic complexity than those of the I-type volcanic–plutonic rock pair. Magmatic zircons from the Hawkins Dacite–Cootralantra Granodiorite pair exhibit a spread of 3·5 ε_{Hf} units, which is well outside of that expected from analytical error. Clearly, these zircons sampled a range of isotopically different melt compositions over their crystallisation interval. The rate of change in ε_{Hf} appears to have been slow relative to the typical growth interval of single zircon crystals, as only one dacite zircon was found to have a clear within-grain Hf isotopic gradient. In this grain, ε_{Hf} decreases strongly towards the rim (from − 7·2 to − 8·5), providing a vector towards a more crustal (lower) melt-$^{176}Hf/^{177}Hf$ with time. Although the spread of $^{176}Hf/^{177}Hf$ ratios overlap within error, the Hawkins Dacite zircons extend to higher ε_{Hf} and have significantly higher average ε_{Hf} values (− 7·8) than the Cootralantra Granodiorite zircons (ε_{Hf} − 9·9). The dacite and granodiorite zircons also occupy different fields on Figure 10. Isotopic differences between zircons of the two rocks are most pronounced on Figure 11, where although ε_{Hf} is weakly (negatively) correlated with $\delta^{18}O$ for both samples, the Hawkins Dacite array is displaced towards higher $\delta^{18}O$ and ε_{Hf}.

The most striking Hf isotope variation is shown by zircons of the S-type Violet Town Ignimbrite–Strathbogie Granite (Fig. 10). Zircon ε_{Hf} values in rhyodacite VT1 range from − 2·7 to +3·3 (average +0·8), markedly higher than in the Hawkins Dacite zircons and high for S-types in general. Zircons in the other rhyodacite sample (VT3) extend to lower ε_{Hf} (1·2 to − 6·9, average − 2·6), so that the total Hf isotope range of these Violet Town Ignimbrite zircons exceeds 10 ε_{Hf} units. Despite this, within-grain isotope variation is subtle and generally not resolvable within the limits of analytical precision (Fig. 8). The Strathbogie Granite zircons also show significant ε_{Hf} dispersion (0·5 to − 6·5), overlapping the range in the ignimbrite (Fig. 10). As is the case for the Hawkins Dacite–Cootralantra Granodiorite samples, zircon ε_{Hf} for the Violet Town Ignimbrite and Strathbogie Granite correlates with $\delta^{18}O$ (Fig. 11), although the ignimbrite and granite zircons define divergent ε_{Hf}–$\delta^{18}O$ trajectories. In the

https://doi.org/10.1017/S0263593300001498 Published online by Cambridge University Press

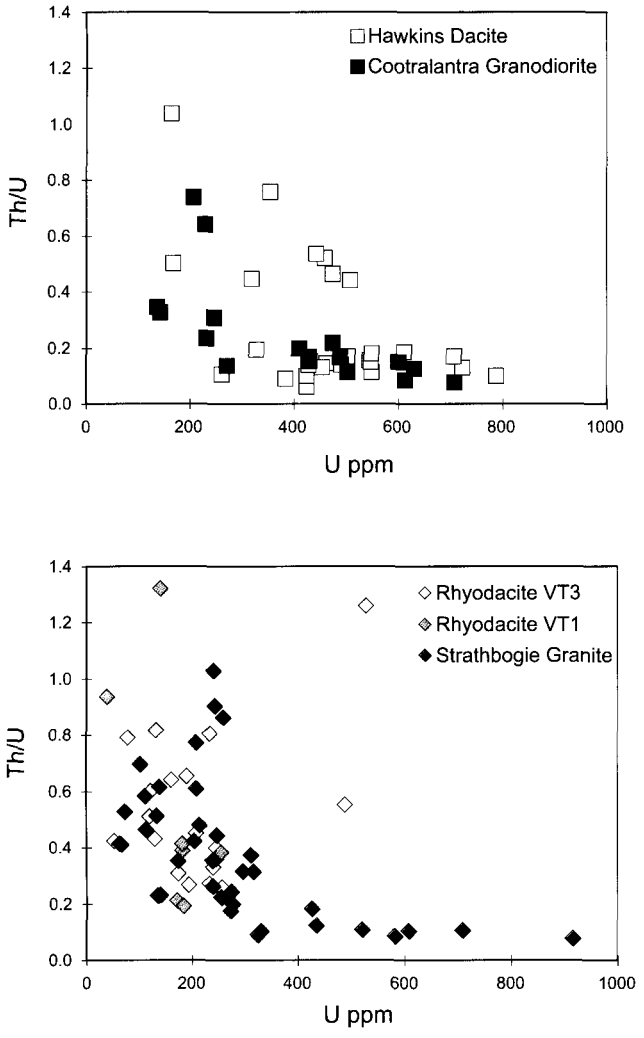

Figure 7 Comparative plots of Th/U versus U content, as measured by ion microprobe, for zircons of the S-type Hawkins Dacite–*Cootralantra Granodiorite (top)* and *Violet Town Ignimbrite*–Strathbogie Granite (bottom, includes data from the Strathbogie Granite sample of Bierlein *et al.* 2001).

Strathbogie Granite zircons, $\delta^{18}O$ increases with ε_{Hf}, this trend being largely controlled by one point with unusually high $\delta^{18}O$ and radiogenic $^{176}Hf/^{177}Hf$. The ignimbrite zircon array overlaps that of the granite zircons at low ε_{Hf}, but shows a systematic fall in $\delta^{18}O$ with increasing ε_{Hf}. These contrasting trends suggest that the Hf–O isotope evolution in the ignimbrite and granite magmas was, at least in part, distinct. Notably, the Strathbogie Granite zircon with the lowest $\delta^{18}O$ and relatively high ε_{Hf} falls within the ignimbrite array.

4. Implications for magma generation processes and the volcanic–plutonic nexus

A detailed petrogenetic study of the LFB granitic and volcanic rocks is beyond the scope of the present paper. The following discussion will instead focus on how the zircon isotope data can shed fresh light on the source materials and processes involved in magma generation, and on the relationship between the plutonic and extrusive units.

4.1. Kadoona Dacite–Glenbog Granodiorite (I-type)

Magmatic zircons within the Kadoona Dacite and Glenbog Granodiorite are coeval and exhibit a limited, overlapping range of O and Hf isotope values, providing additional support for a broadly co-magmatic relationship between these volcanic and granitic units (Wyborn & Chappell 1986; Chappell *et al.* 1987). The data imply that the respective magmas formed from similar source materials; the bulk rock chemical differences between the specific samples analysed here might be due to a greater accumulation of melt-precipitated and/or restitic crystals in the erupted magma compared to that which solidified in the plutonic environment.

Insight into the nature of the magma sources is provided by the O isotope data. The key issue concerns the elevated $\delta^{18}O$ in zircons from the Kadoona Dacite and Glenbog Granodiorite. The composition-$\Delta^{18}O$ relationship for magmatic zircons predicts that zircons in these rocks would crystallise from melts with $\delta^{18}O$ of around 8–9·5‰, in good agreement with the measured whole-rock $\delta^{18}O$ of the granodiorite. However, this is too high for I-type magmas believed to be derived from basaltic/andesitic precursors and testifies to a substantial supracrustal component in both the Kadoona Dacite and Glenbog Granodiorite. The elevated $^{87}Sr/^{86}Sr$ and low ε_{Nd} of the Glenbog Granodiorite (Fig. 3) probably also reflects this supracrustal ingredient to some extent, rather than the crustal residence age of a mafic protolith. Chappell & Stephens (1988) suggested that the high bulk rock $\delta^{18}O$ values reflect introduction of supracrustal material into the meta-igneous precursors of the LFB I-type plutons during a prior episode of sea-floor weathering and subduction. A similar scenario has recently been proposed for high $\delta^{18}O$ metaluminous plutons of the Sierra Nevada Batholith (Lackey *et al.* 2005). However, the present authors favour a direct sedimentary input into the LFB I-type magmas, since (1) the I-type suites contain inherited zircons of similar age to detrital zircons in the metasedimentary country rocks; (2) there is clear field evidence for metasedimentary rock assimilation at the base of I-type batholiths (e.g. Kemp *et al.* 2005b); and (3) the collective zircon arrays defined by the I-type granites project towards the Hf–O isotope composition of the Ordovician metasedimentary basement, and the Hf–O isotope systematics of the Kadoona Dacite–Glenbog Granodiorite zircons are consistent with these trends (Fig. 12). The subtle ^{18}O enrichment in the dacite zircons relative to the granodiorite zircons suggests a slightly greater supracrustal input into the erupted magma. Whether this difference, and the combined $\delta^{18}O$ range of the Kadoona Dacite–Glenbog Granodiorite zircons evident in Figure 12, reflects mixing processes like those described by Kemp *et al.* (2007) should be resolved by analysis of zircons from other samples of these units. The Kadoona Dacite and Glenbog Granodiorite cannot be regarded as strictly 'infracrustally-derived' (I-type) in the original usage of Chappell & White (1974), despite their metaluminous character.

4.2. Hawkins Dacite–Cootralantra Granodiorite (S-type)

The wide ranges of ε_{Hf} values and associated shifts in $\delta^{18}O$ shown by zircons of the S-type granitic/volcanic pairs are only reconciled by open-system evolution, that is, by the operation of processes capable of changing the $^{176}Hf/^{177}Hf$ and $^{18}O/^{16}O$ ratios of the magma during zircon crystallisation. Change of this nature, whilst long suspected in the genesis of S-type granites (Gray 1984, 1990; Elburg & Nicholls 1995; Maas *et al.* 1997; DiVincenzo *et al.* 1996; Castro *et al.* 1999; Healy *et al.* 2004) has proved difficult to establish by whole rock methods. Microsampling of magmatic feldspar did reveal some syn-magmatic isotopic variation in samples of the S-type Wilson's Promontory Batholith (Waight *et al.* 2000), but extrapolation to the whole rock, let alone pluton-scale, was problematic. The Hf–O isotope data from melt-precipitated zircons represents the most compelling evidence to date that models seeking to explain the geochemical evolution of these rocks solely by

https://doi.org/10.1017/S0263593300001498 Published online by Cambridge University Press

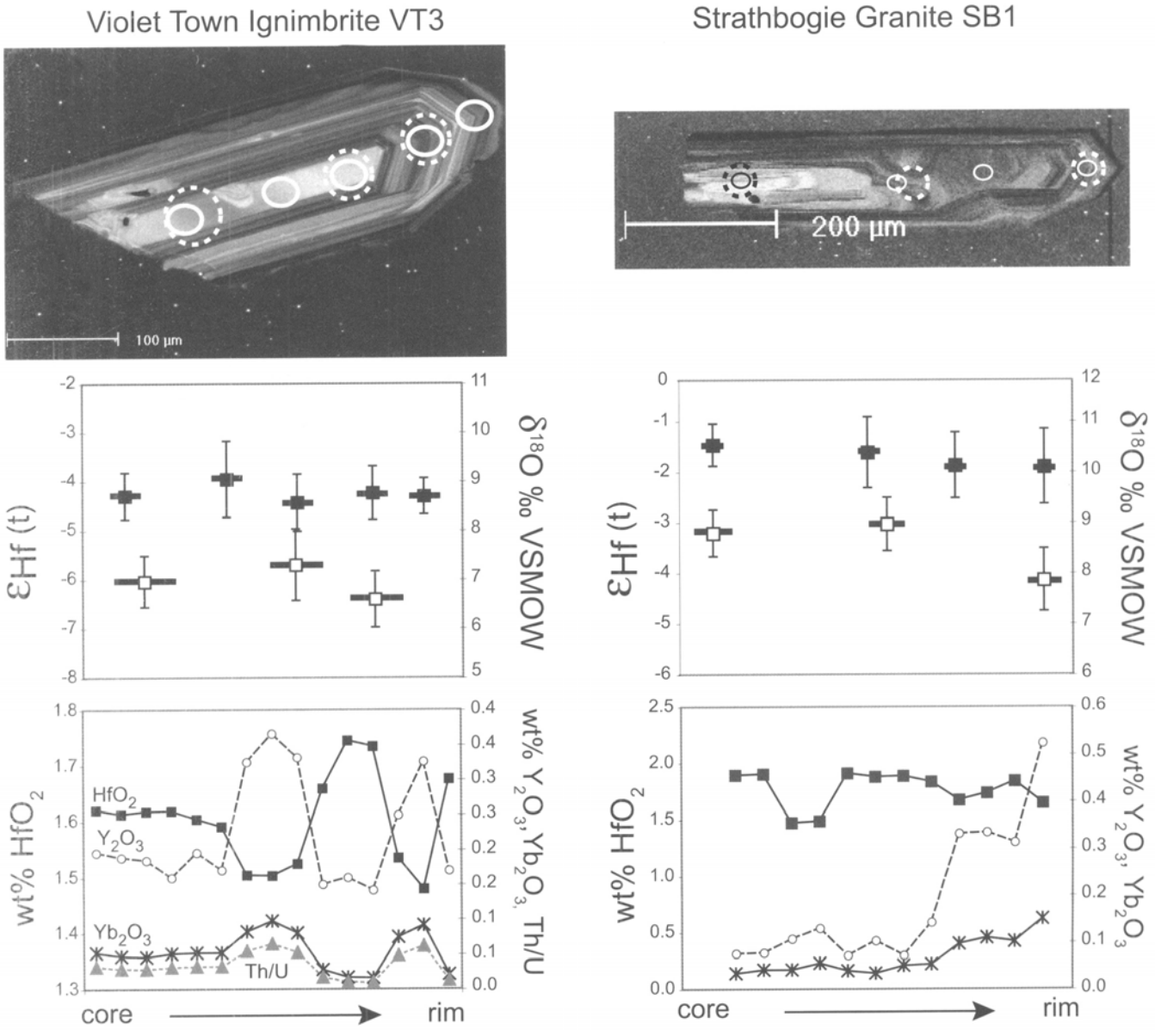

Figure 8 Trace element and Hf–O isotope characteristics of magmatic zircons in samples of the Violet Town Ignimbrite (left) and Strathbogie Granite (right). The bottom panel shows core-rim electron microprobe traverses for HfO_2, Y_2O_3 Yb_2O_3, and Th/U (Th contents were mostly below detection for SB1), whereas the top panel shows the Hf (open symbols) and O (closed symbols) isotope composition determined for the same part of each crystal; the horizontal bar depicts the approximate spatial resolution of the isotope analyses in relation to the electron probe traverse. Error bars are shown at 2 s.e.

crystal-liquid separation (e.g. Clemens & Wall 1984; Chappell *et al.* 1987) are incomplete.

The covariant ε_{Hf}–$\delta^{18}O$ arrays defined by the studied S-type zircons indicate mixing between two contrasting components. The main tasks now are to establish the nature of these components, and to identify the polarity of isotope change during magmatic evolution (i.e. whether ε_{Hf} increases or decreases during zircon crystallisation). Although intra-zircon Hf–O isotope zoning is virtually absent, a sense of the direction of change may be gleaned from Th/U ratios. For melt-precipitated zircons of the Hawkins Dacite, the ε_{Hf} values display a positive correlation with the Th/U ratio measured from the same part of each crystal (Fig. 13). Since the Th/U ratios exhibit a systematic core-rim decrease for zircons of this sample (established by ion microprobe and electron probe analysis), it is tentatively inferred that the $^{176}Hf/^{177}Hf$ of the dacite magma generally decreased with crystallisation. The isotope evolution of the Hawkins Dacite thus involved interaction between a parental magma and a source component with lower ε_{Hf}, and higher $\delta^{18}O$. The Ordovician metasedimentary country rocks conceivably represent the latter; localised anatexis of these materials resulted in the formation of small diatexitic plutons whose bulk rock isotope compositions anchor the high initial $^{87}Sr/^{86}Sr$ end of the Sr–Nd isotope array defined by the eastern LFB granites (McCulloch & Chappell 1982; Gray 1984; Fig. 3). The identity of the parental high ε_{Hf} magma is less well constrained. Possibilities include either a crustal melt derived from a feldspathic, perhaps volcanogenic greywacke (see Clemens 2003), an I-type tonalitic magma (Collins 1996) or even a basaltic magma (Gray 1984). Dark coloured, igneous-textured enclaves could manifest a relatively juvenile magmatic input into the LFB S-type plutons (Vernon 1991), but the extent to which this process influences the composition of the host granite is debateable (e.g. Clemens 2003).

Figure 14 explores the relations between Hf and O isotopes in the analysed S-type magmatic zircons, and seeks to explain them in terms of different mixing arrays. Both binary mixing

https://doi.org/10.1017/S0263593300001498 Published online by Cambridge University Press

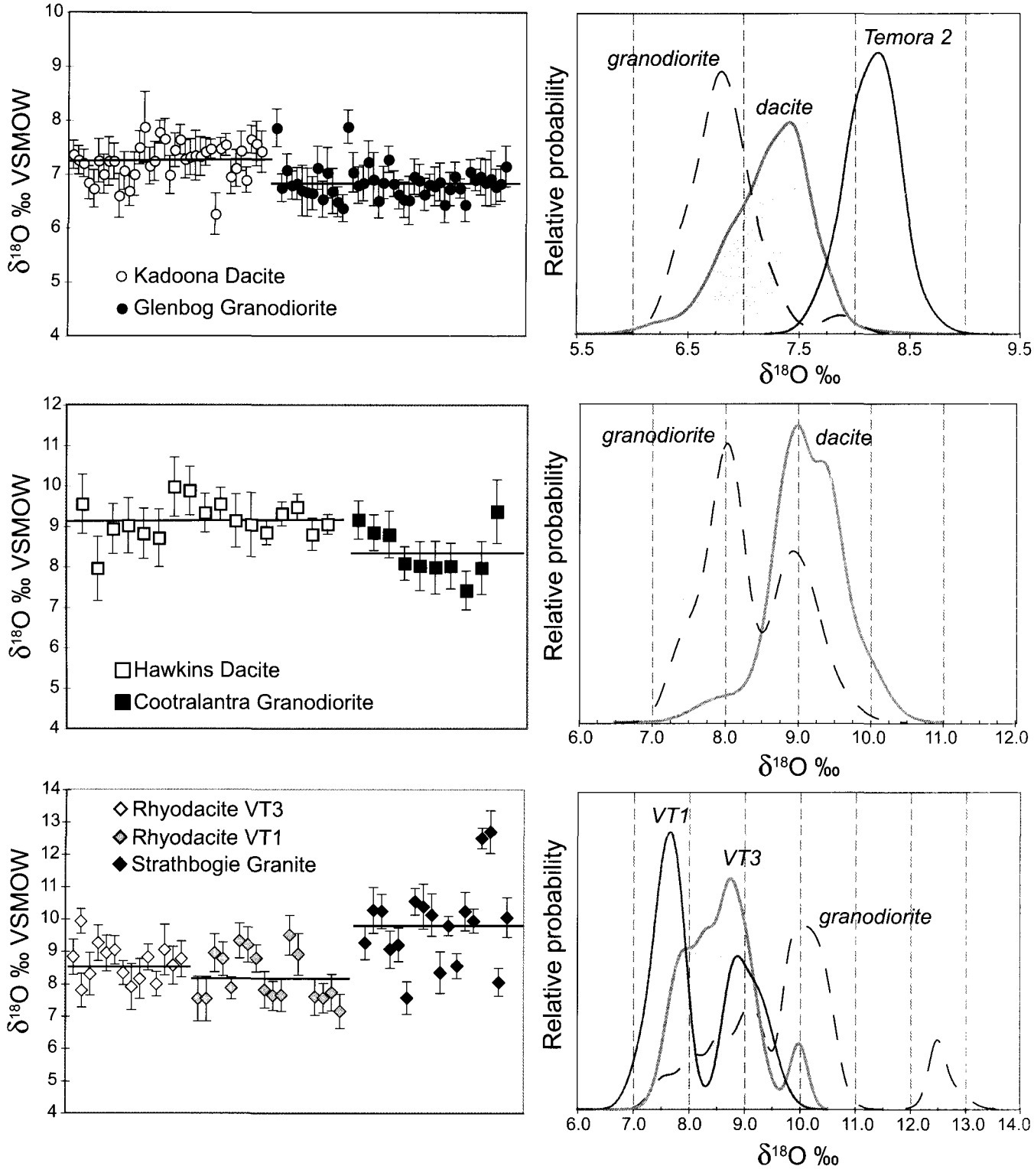

Figure 9 Oxygen isotope composition of zircons from the three volcanic–plutonic rock pairs plotted as individual analyses (left, horizontal bars denote the average zircon $\delta^{18}O$ values for each sample) or probability density functions (right). Error bars are shown at 2 σ and reflect counting statistics as well as the standard deviation of the bracketing standard zircon analyses. The probability density function defined by twenty analyses of zircon standard Temora 2 is shown at the top right for comparison. These Temora 2 analyses were obtained in a single analytical session and yielded an average $\delta^{18}O$ value of 8·2 ± 0·2‰ (1 s.d.) identical to the laser fluorination value quoted by Valley (2003).

and coupled assimilation-fractional crystallisation (AFC) formulations are employed. The curvature of these arrays is controlled by the Hf/O elemental ratios of the end-member components; however, because oxygen contents tend to be similar in most rocks/melts, it is essentially the Hf concentrations of the end-member components that determine the shape of the mixing curves. It was emphasised at the outset that these scenarios are inevitably approximations for complex igneous systems (and variables such as D_{Hf} and Hf content are difficult to constrain), but they serve to highlight the processes that could generate zircon Hf–O isotope arrays during magmatic evolution.

For the Hawkins Dacite–Cootralantra Granodiorite, mixing calculations assume that the parental high ε_{Hf} magma was

https://doi.org/10.1017/S0263593300001498 Published online by Cambridge University Press

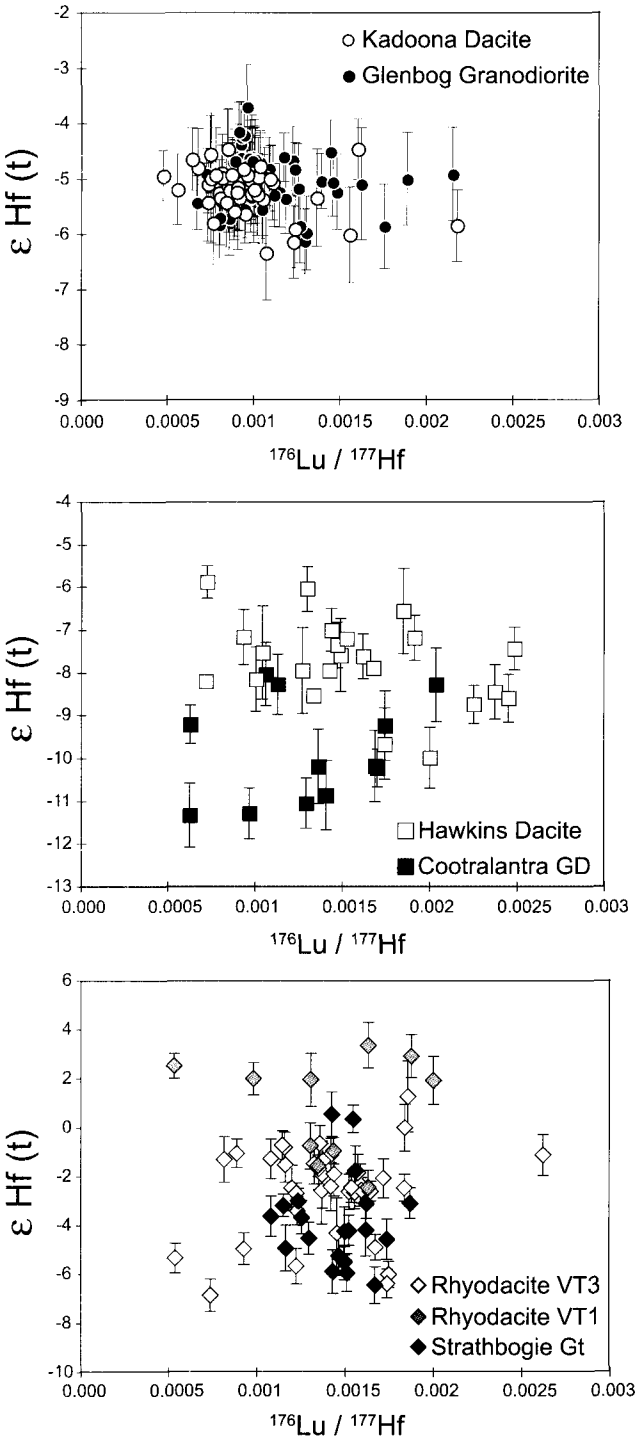

Figure 10 Plots of ε_{Hf} (calculated at the crystallisation age) versus $^{176}Lu/^{177}Hf$ for zircons of the Kadoona Dacite–Glenbog Granodiorite, Hawkins Dacite–Cootralantra Granodiorite and Violet Town Ignimbrite–Strathbogie Granite (2 s.e. error bars are indicated).

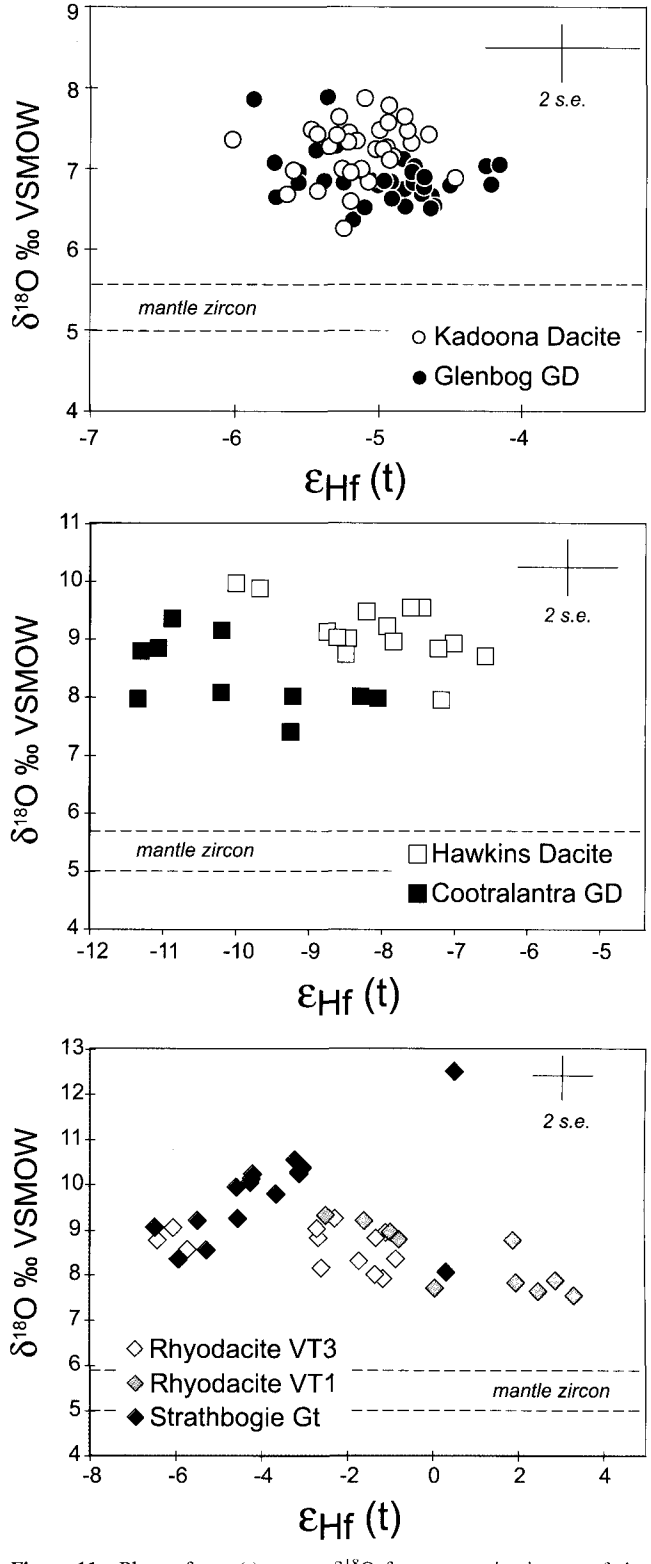

Figure 11 Plots of ε_{Hf} (t) versus $\delta^{18}O$ for magmatic zircons of the three volcanic–plutonic rock pairs (average 2 s.e. error bars are indicated. GD, granodiorite; G, granite). The dashed lines encompass the $\delta^{18}O$ range of zircon in equilibrium with mantle oxygen (Valley 2003).

isotopically analogous to the Blind Gabbro, a mafic pluton that is spatially associated with the S-type rocks of the Bullenbalong Supersuite in the eastern LFB (Hine *et al.* 1978). Whilst it is unclear if this particular gabbro played a role in S-type granite petrogenesis, it is nevertheless useful as a proxy for Silurian basaltic components in the region, and zircon Hf–O isotope data are available from Kemp *et al.* (2007). In the model shown in Figure 14, the zircons in the Hawkins Dacite magma may have crystallised from melts generated by hybridisation between gabbroic magma and metasedimentary-derived material, involving either 40–65% AFC or 60–85% simple mixing. The geometry of the mixing curves require that the metasedimentary component had relatively low Hf content, which could apply to a partial melt in equilibrium with residual zircon. The high inferred degree of supracrustal input is most consistent with deep crustal mixing/assimilation involving hot, parental liquids, rather than country-rock contamination in shallow level magma chambers (Thompson *et al.* 2002). The Hf–O isotope compositions of zircons from a nearby I-type tonalite also plot along the same trajectory as the dacite

https://doi.org/10.1017/S0263593300001498 Published online by Cambridge University Press

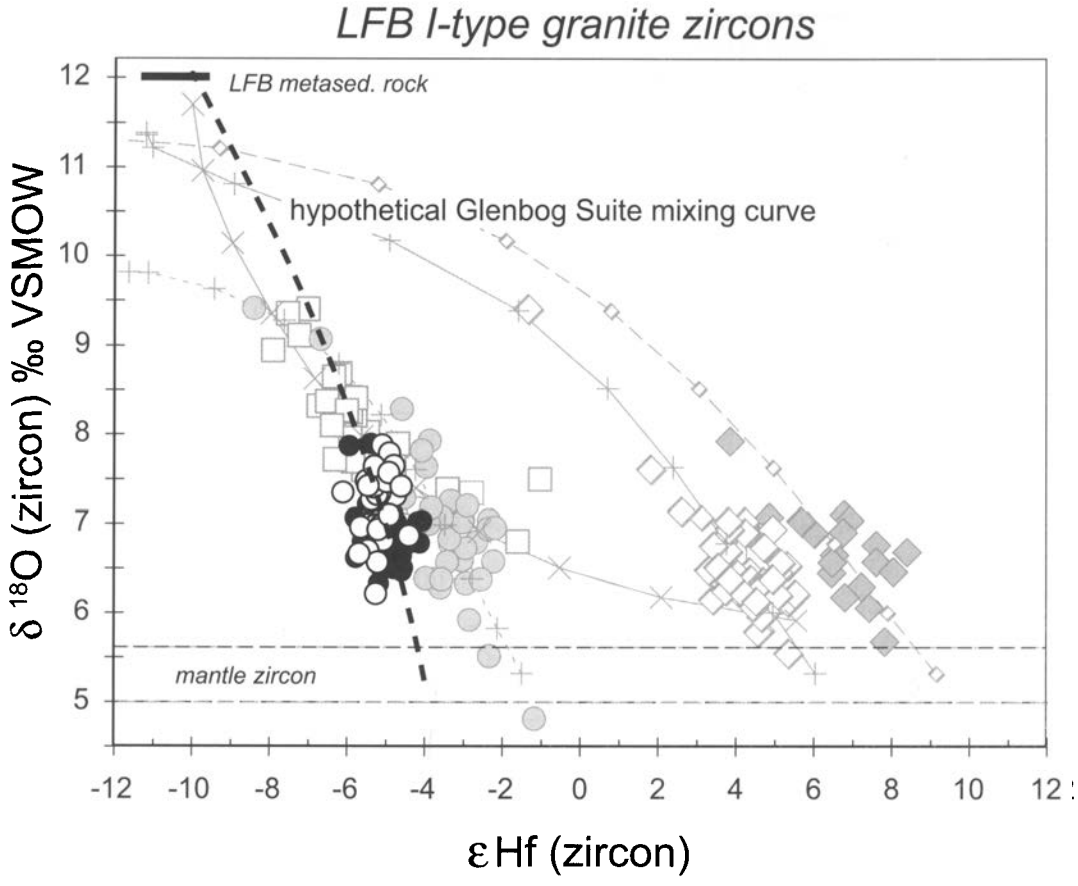

Figure 12 The Hf–O isotope systematics of zircons from the Kadoona Dacite and Glenbog Granodiorite (symbols as in Figure 9) compared to the isotope composition of zircons from other I-type granites of eastern Australia (Jindabyne Suite, circles; Why Worry Suite, squares, Cobargo Suite, diamonds; from Kemp *et al.* 2007). Further study is required to determine whether the Kadoona Dacite/Glenbog Granodiorite zircons comprise part of a wider mixing array (dashed curve).

zircons (Fig. 14), supporting the idea that the LFB I- and S-type granites comprise part of the same mixing system (Gray 1984; Collins 1996). The concave-upwards Hf–O isotope trend of the Cootralantra Granodiorite can be reproduced with the same source components, but using a higher Hf content for the ^{18}O-enriched material, as might be the case for bulk mixing or assimilation of metasedimentary rock. On this basis, it is speculated that the differences between the Hawkins Dacite and the Cootralantra Granodiorite reflect the manner in which the low ε_{Hf} metasedimentary component was incorporated. The greater thermal demands of bulk mixing might have caused the stalling and crystallisation of the S-type magma in the upper crust, resulting in granodiorite pluton formation.

4.3. Violet Town Ignimbrite–Strathbogie Granite (S-type)

Like the Hawkins Dacite/Cootralantra Granodiorite example, the Violet Town Ignimbrite magma also evidently evolved towards a more 'crust-like' isotope composition with time. This is supported by the following observations: (1) the basal high silica rhyolite unit of the ignimbrite sequence, presumably erupted first, has significantly more primitive bulk rock Nd isotope ratios than the overlying rhyodacites (Elburg 1996); and (2) zircons in the stratigraphically higher rhyodacite (VT3) have, on average, lower ^{176}Hf/^{177}Hf. The evolution towards lower ε_{Hf} and higher δ^{18}O is extended in the slightly younger Strathbogie Granite. The overall ε_{Hf} decrease for all three rocks may be viewed as a secular trend in this silicic igneous complex. Another manifestation of this trend may be the general positive correlation between zircon Th/U ratios and ε_{Hf} (Fig. 13). The Violet Town Ignimbrite is peraluminous, but a juvenile precursor is plausible since the zircon Hf–O isotope arrays clearly project to a mantle-like composition (Fig. 11). The quenched basaltic andesite enclaves within the rhyodacite are evidence for coeval mafic magmatism (Elburg 1996).

One way in which such a Hf–O isotope trend can arise is by melt extraction from a magma reservoir at depth that is becoming increasingly contaminated by supracrustal materials. The overall process may resemble the 'hot zone' scenario envisaged by Annen & Sparks (2002) and Annen *et al.* (2006), involving the repeated injection of basaltic sills into the lower to middle crust. Here, silicic melts are generated both by fusion of the adjacent crustal rocks and as residual liquids from basalt crystallisation, with the relative proportions being governed by the rate and depth of sill emplacement, the initial basalt temperature and H_2O content, and the fertility of the crustal rocks (Annen & Sparks 2002). Simulations predict that silicic melts first accumulate within the intruded basalt pile, but that anatectic melt production in the overlying crustal rocks increases rapidly thereafter, especially where the basalt is hot and dry (Annen & Sparks 2002). Mingling or mixing between the disparate melt aliquots extracted from each layer is inevitable, conceivably generating magmatic products whose isotope ratios become more crust-like with time. The present authors suggest that the isotope systematics of zircons within the Violet Town Ignimbrite manifest such a process. The ε_{Hf}–δ^{18}O arrays of the rhyodacite zircons can be modelled by the progressive mixing or assimilation of partial melt from the Ordovician metasedimentary rocks and residual silicic liquid derived from a parental basaltic magma (20–45% AFC or

https://doi.org/10.1017/S0263593300001498 Published online by Cambridge University Press

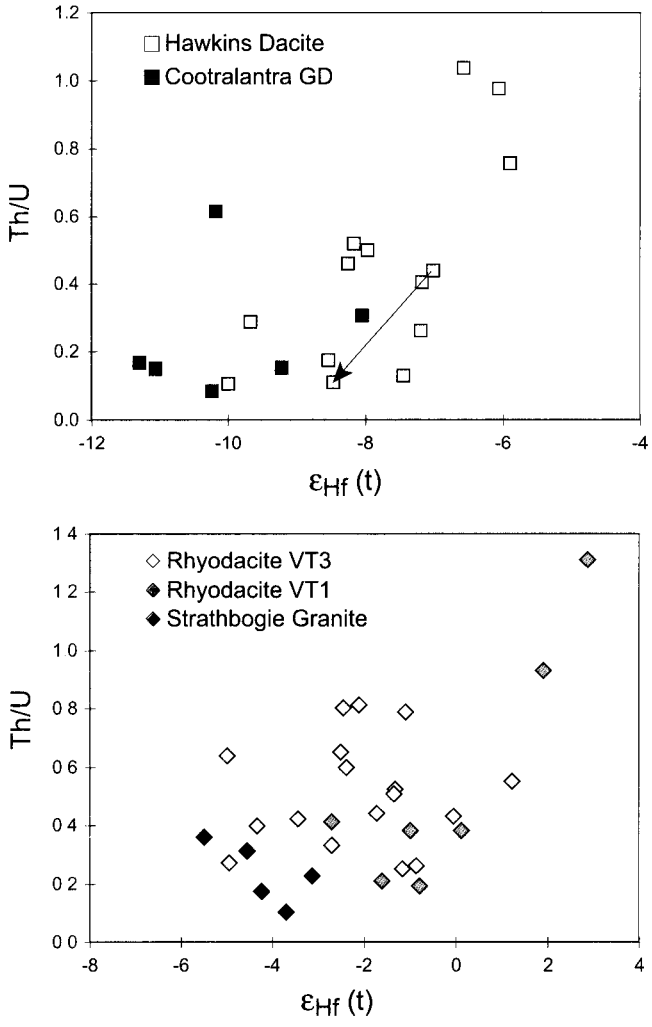

Figure 13 Plot of ε_{Hf} (t) versus Th/U for zircons of the Hawkins Dacite–Cootralantra Granodiorite (top) and Violet Town Ignimbrite–Strathbogie Granite (bottom) (Th/U was measured by ion microprobe). Data are only shown for cases where the Hf isotope data were acquired by directly ablating the ion microprobe pit. Th/U ratios show an overall decrease towards the rim for all zircons. The arrowed tie line connects analyses from one core-rim pair in the Hawkins Dacite that shows a pronounced difference in ε_{Hf}.

35–75% simple mixing of crustal melt; Fig. 14). An attraction of this model is that the isotopically mantle-like material is not basaltic, which alleviates many of the perceived difficulties with modelling the geochemistry of S-type magmas by crust-mantle mixing (e.g. Chappell *et al.* 1987). The metasedimentary input, in tandem with fractional crystallisation, was presumably sufficient to impart the mildly peraluminous chemistry of the ignimbrite. However, the extent of supracrustal incorporation was significantly less than in the S-type Hawkins Dacite, which has a greater proportion of inherited cores and lower ε_{Hf} in its eruption-age zircon crystals.

While the model suggested above seems capable of explaining the overall secular trend towards lower ε_{Hf} in the igneous complex, it is notable that the zircon Hf–O isotope data for the granitic sample define a trend that projects away from the Violet Town Ignimbrite zircon Hf–O array (Fig. 11). At its low ε_{Hf} end, the Strathbogie Granite zircon array is anchored in the ignimbrite trend, presumably reflecting the continuation of the deep-seated melting/mixing process; the higher bulk rock A.S.I. and lower average $^{176}Hf/^{177}Hf$ in the Strathbogie Granite zircons reflect a greater contribution from metasedimentary source materials. However, the distinctive trend towards higher $\delta^{18}O$ *and* ε_{Hf} requires an additional source component with an unusual isotopic composition. One possibility is that this trend reflects the late stage bulk assimilation of altered volcanic units with high $\delta^{18}O$ and ε_{Hf} by the granite magma as it intruded the base of the ignimbrite sequence. AFC modelling based on this process can account for much of the isotope Hf–O dispersion shown by the Strathbogie Granite zircons (Fig. 14), assuming a low assimilation/crystallisation ratio and using the highest whole-rock $\delta^{18}O$ for the ignimbrite reported by Elburg (1996). The true $\delta^{18}O$ of the basal volcanic sequence, which includes rhyolitic agglomerates, was conceivably much higher, and this would diminish the amount of assimilation required. The Strathbogie Granite zircon with the lowest $\delta^{18}O$ may be a xenocryst incorporated from the ignimbrite. In summary, although the zircon isotope arrays in the Violet Town Ignimbrite and Strathbogie Granite are not identical, these units can be linked by a combination of near-source and shallow crustal open-system differentiation processes.

4.4. Implications for pluton assembly and granite geochemistry

An intriguing aspect of the S-type zircon data concerns the large range of $^{176}Hf/^{177}Hf$ values consistently recorded by zircons of the same sample (see also Kemp *et al.* 2007). This implies that each rock represents an amalgamation of crystals formed from very different melt compositions, and potentially at different times. The virtual absence of discernible intracrystal Hf–O isotope zoning further suggests that either the crystallisation of individual zircons was rapid compared to the rate of isotopic change in the magmatic system overall, and/or that the zircons crystallised from isolated melt pockets within a heterogeneous, poorly mixed magma. All of these features can be explained by incremental proto-pluton formation in response to the deep-seated differentiation process outlined above. Such a scenario would involve discrete batches of magma periodically ascending from the differentiation zone, to crystallise in the upper crust (e.g. Bons *et al.* 2004). Successive magma pulses would then arrive to crystallise isotopically distinct zircons, their Hf–O isotope signature being determined by the extent of mixing between the newly emplaced melt and the resident magma. The trace element fluctuations in zircon grains (Figs 6, 8) could reflect cycling through melt batches that had experienced different degrees of crystallisation, or (where not accompanied by isotope zoning) they might be due to local kinetic or crystal-chemical effects (e.g. Hoskin 2000). Provided that the supply-rate remains high, the growing magma reservoir can remain partially melted, permitting mixing and juxtaposition of zircons with different petrogenetic histories by accumulation or other crystal-liquid sorting process, or convective self-mixing within crystal mushes (Couch *et al.* 2001). Eruption is another efficient way to entrain and mix crystals from different parts of a heterogeneous magma chamber (e.g. Vasquez & Reid 2005).

This model has several implications. First, it suggests that the phenocryst assemblages of silicic igneous rocks may not be related through a common melt composition, as increasingly recognised from other lines of petrological and isotope evidence (e.g. Bachmann *et al.* 2002; Davidson *et al.* 2005). This means that magmatic P–T estimates based on exchange equilibria between coexisting phenocryst phases are potentially spurious, as these minerals may not have crystallised in equilibrium but owe their association to late-stage physical accumulation. For example, we show here that zircon crystals in each S-type ignimbrite sample were in equilibrium with melts that were up to 6 ε_{Hf} units different, and it seems inevitable that the temperature and geochemistry of these melts were also different. The extent to which such contrasts

https://doi.org/10.1017/S0263593300001498 Published online by Cambridge University Press

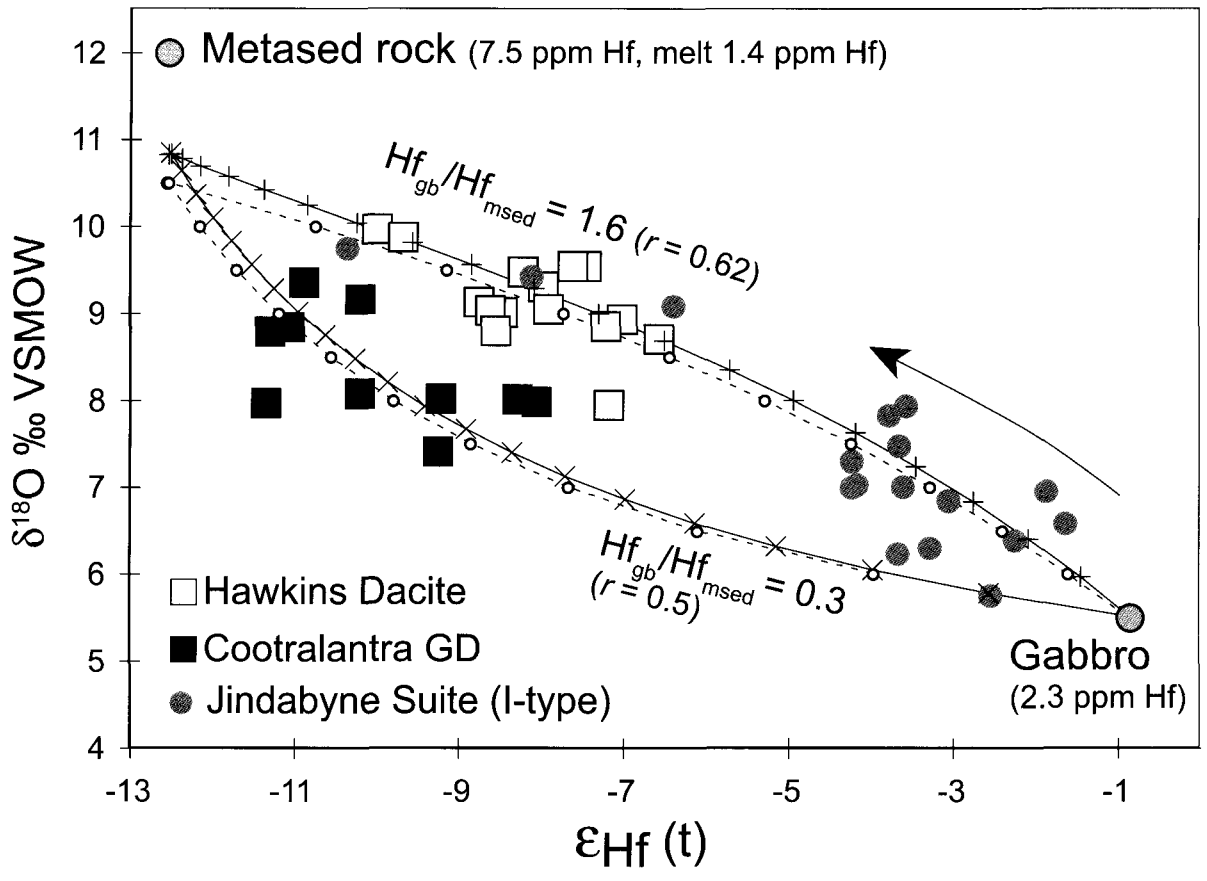

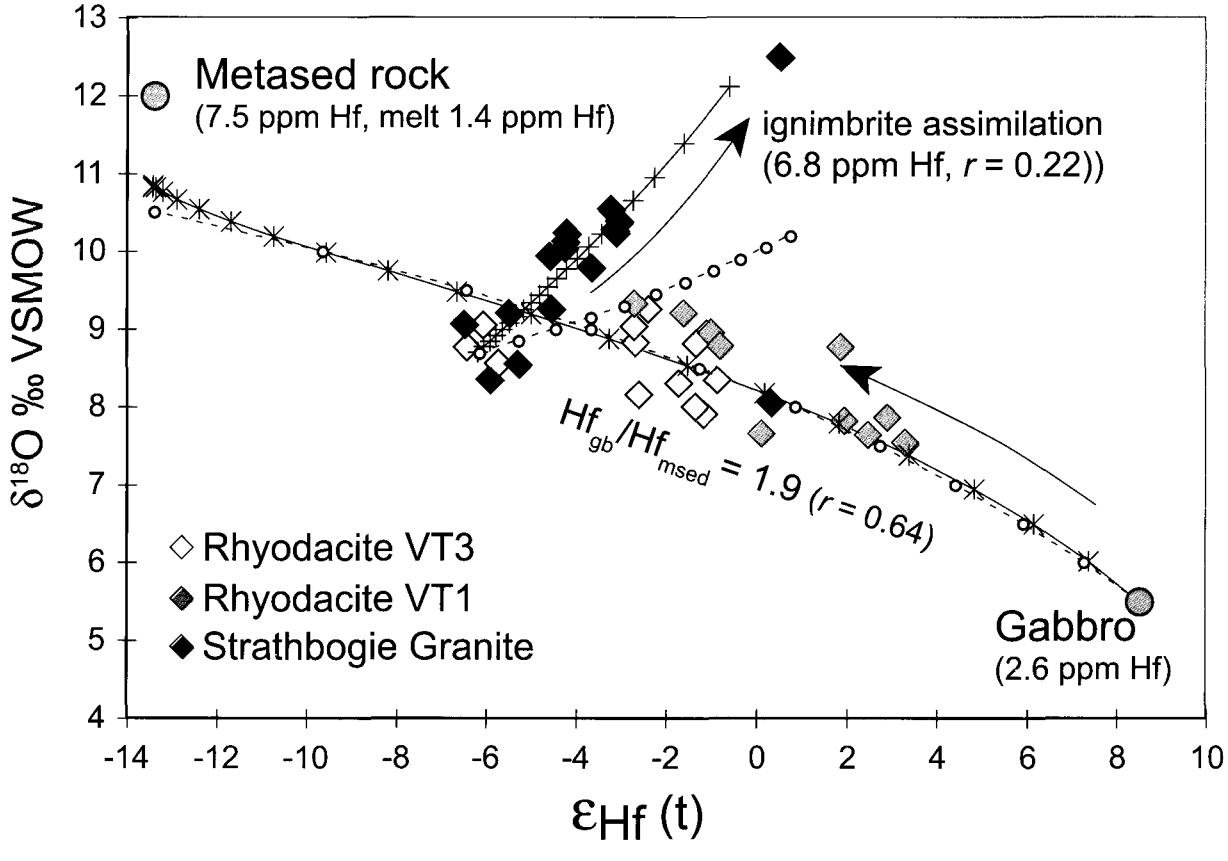

https://doi.org/10.1017/S0263593300001498 Published online by Cambridge University Press

are maintained at magmatic conditions obviously depends on inter- and intra-mineral diffusion rates, which are low for Hf (Cherniak *et al.* 1999) and O (Peck *et al.* 2003) in zircon. Investigation of the isotope systematics of zircon inclusions in co-existing phenocrysts may help assess the relationship between these phases, by determining the stage in the magmatic evolution at which the phenocrysts originally crystallised.

Secondly, the model implies that the bulk geochemistry of granitic-volcanic rocks is strongly influenced by crystal-liquid processes in upper crustal magma reservoirs, such as filter pressing and crystal accumulation. Outcrop evidence for such behaviour abounds in felsic plutonic rocks (Wiebe & Collins 1998; Weinberg 2006), and this can contribute towards the characteristic linear geochemical variation shown by granitic suites. Annen & Sparks (2002) proposed that the textural characteristics of silicic igneous rocks reflect shallow level crystallisation, and the present authors suggest that much within-pluton geochemical diversity arises here as well. In contrast, the isotope systematics and overall geochemical attributes of the parental magmas (such as incompatible trace element ratios) are determined by open-system differentiation in the deep crust, involving the participation of disparate crustal and mantle-derived components (Annen *et al.* 2006; Kemp *et al.* 2007). These effects, which work to decouple elemental and isotopic compositions, can confound attempts to model the geochemical trends of granite suites in terms of isotopically defined source components.

4.5. Implications for the origin of phenocrysts in volcanic rocks

Phenocrysts in the LFB volcanic rocks have been interpreted as refractory or restitic (including peritectic reaction products) minerals entrained from the magma's source region (e.g. Chappell *et al.* 1987). However, some phenocrysts encapsulate oscillatory and sector-zoned eruption-age magmatic zircons. If phenocryst growth is indeed a magma source phenomenon, it would require that phenocrysts were growing during the melting process at the same time that zircon was precipitating from the melt. This appears unlikely, given the trace element heterogeneity of the zircons (e.g. Th/U), which implies sampling of diverse melt compositions, and elongate, sector-zoned zircon morphologies, which suggest rapid crystallisation (Corfu *et al.* 2003). The preferred alternative is that at least some portion of the phenocryst population crystallised at shallow crustal levels, possibly induced by decompression and degassing (Cashman & Blundy 2000). The zircons may have adhered to resorption surfaces on restitic and/or xenocrystic minerals, to be subsequently overgrown. This interpretation agrees with the preponderance of zircon inclusions in cordierite and orthopyroxene, phases whose crystallisation is favoured at low pressure (Clemens & Wall 1981; Vielzeuf & Montel 1994), and absence of zircon inclusions in garnet and quartz, both of which show evidence for decompression-related reaction (garnet) or resorption (quartz).

5. Conclusion

The U–Pb, O and Hf isotopic diversity in melt-precipitated zircons within LFB volcanic rocks and their inferred plutonic analogues suggests complex petrogenetic histories, despite the similarity in whole rock compositions. However, the data cement, rather than compromise the volcanic–plutonic link, as the respective magmas have apparently followed similar evolutionary pathways.

The I-type dacite–granodiorite pair presents the simplest case. The similar zircon isotope systematics of these rocks suggests that the dacite is the extrusive equivalent of the granodiorite, as originally proposed by Wyborn & Chappell (1986). The subtle bulk-rock geochemical differences between these samples thus probably reflect crystal-liquid processes. Zircons of both samples have elevated $\delta^{18}O$ relative to that of mantle-derived materials, requiring a significant supracrustal source ingredient.

The major conclusion from the S-type zircon data is that, through covariant ε_{Hf}–$\delta^{18}O$ arrays, these grains are registering the interaction between two contrasting components during magmatic evolution. The petrological and compositional characteristics of the S-type granitic/volcanic rocks cannot therefore be explained in terms of a specific protolith composition. The data instead suggest that the S-type magmas formed through the progressive incorporation (by mixing or assimilation) of high $\delta^{18}O$ material, perhaps similar to the Ordovician metasedimentary country rocks, by relatively primitive magmatic parents. Thermal considerations predict that digestion of supracrustal materials would be most efficient at depth in response to regional temperature anomalies caused by mafic magma under- and intra-plating. The spectrum of Hf–O isotope ratios shown by zircons of the same rock sample indicate the physical juxtaposition of crystals that formed at very different stages of magmatic evolution, either during crystal-liquid sorting in shallow magma reservoirs or during eruption. Trends between element–element pairs on variation diagrams can originate in this way. In such a situation, the bulk rock geochemical trends and isotope variations of silicic igneous suites are decoupled, as they reflect essentially independent processes operating at different crustal levels. This can explain mismatches between the observed granite geochemistry and that predicted using end-member components inferred from whole-rock isotope data.

Figure 14 The ε_{Hf}–$\delta^{18}O$ isotope arrays of zircons from the S-type suites compared to the model isotopic trajectories produced by binary mixing (dashed line) and assimilation-fractional crystallisation (solid line, equation from DePaolo 1981) involving various crustal and mantle-derived source materials. Zircon isotope data from the I-type Jindabyne Suite (filled grey circles) are shown for comparison. The inferred overall direction of magmatic evolution is arrowed. The model curves were corrected for zircon/magma fractionation assuming a linear change in $\Delta^{18}O_{Zrc\text{-}WR}$ from $-0{\cdot}5‰$ to $-1{\cdot}5‰$ during the mixing/assimilation process (except for the Strathbogie Granite zircon trend, where $\Delta^{18}O_{Zrc\ WR}$ was kept constant at $-1{\cdot}5‰$). The D_{Hf} values were computed from mineral modes and partition coefficients in the 'Earthref' database (www/earthref.org). The 'ignimbrite assimilation' trend for the Strathbogie Granite zircons was modelled using the average $^{176}Hf/^{177}Hf$ of the rhyodacite assimilant and a $\delta^{18}O$ of 11·7‰ (from Elburg 1996). Isotope values used for the Ordovician metasedimentary rocks were $\delta^{18}O$ 12‰ (O'Neil & Chappell 1977) and $^{176}Hf/^{177}Hf$ 0·28215, estimated from the relationship between ε_{Nd} and ε_{Hf} for a global database of terrestrial rocks (Vervoort *et al.* 1999). The isotope composition of the low $\delta^{18}O$ component of the Violet Town Ignimbrite magmas was estimated from data in Soesoo (2000) for mafic rocks of the central LFB. Data for the Blind Gabbro zircons are from Kemp *et al.* (2007). The Hf concentrations adopted in the calculations were derived from bulk rock data (assuming a chondritic Zr/Hf for mafic rock analyses in Soesoo 2000). Values for the rate of assimilation to fractional crystallisation (r) were iteratively chosen so as to produce the optimum visual fit to the zircon isotope data.

https://doi.org/10.1017/S0263593300001498 Published online by Cambridge University Press

Further work is required to test and refine the petrogenetic models for the LFB granitic and volcanic rocks presented herein. Nevertheless, this study highlights the potential for the combined Hf–O isotope variations in zircon to provide important insights into the processes of silicic magma generation and evolution. This approach could prove particularly fruitful for high-level volcano–plutonic systems, since $^{18}O/^{16}O$ is sensitive to flux infiltration from degassing magmas at depth, interaction with meteoric waters near the volcanic edifice, and recycling of previously erupted material (Valley 2003), whereas Hf isotopes diagnose input from older crust. Zircon-hosted isotope tracers are relatively impervious to the severe hydrothermal alteration that may affect high-level magmatic systems. Advances are likely to stem from more fully integrating Hf–O isotope data with trace element data, particularly to track crystallisation processes and to place isotope variations into a thermal context using Ti-in-zircon thermometry (Watson & Harrison 2005), and in young silicic igneous rocks where the temporal framework of zircon crystallisation can be more precisely established.

6. Acknowledgements

We appreciate the patience of the editors of this volume during TK's island hopping while preparing this manuscript. The electron microprobe data was acquired with the assistance of Stuart Kearns and Jon Wade, and Chris Coath was instrumental in setting up the isotope laboratories at the University of Bristol. John Craven was specifically responsible for developing techniques for oxygen isotope analysis at Edinburgh. The manuscript benefited from constructive reviews by Jon Davidson and Calvin Miller.

7. References

Annen, C., Blundy, J. D. & Sparks, R. S. J. 2006. The genesis of intermediate and silicic magmas in deep crustal hot zones. *Journal of Petrology* **47**, 505–39.

Annen, C. & Sparks, R. S. J. 2002. Effects of repetitive emplacement of basaltic intrusions on thermal evolution and melt generation in the crust. *Earth and Planetary Science Letters* **203**, 937–55.

Bachmann, O., Dungan, M. A. & Lipman, P. W. 2002. The Fish Canyon magma body, San Juan volcanic field, Colorado: rejuvenation and eruption of an upper-crustal batholith. *Journal of Petrology* **43**, 1469–503.

Bachmann, O. & Bergantz, G. W. 2004. On the origin of crystal-poor rhyolites: extracted from batholithic crystal mushes. *Journal of Petrology* **45**, 1565–82.

Belousova, E. A., Griffin, W. L. & O'Reilly, S. Y. 2006. Zircon crystal morphology, trace element signatures and Hf isotope composition as a tool for petrogenetic modeling: examples from Eastern Australian granitoids. *Journal of Petrology* **47**, 329–53.

Bierlein, F. P., Arne, D. C., Keay, S. M. & McNaughton, N. J. 2001. Timing relationships between felsic magmatism and mineralisation in the central Victorian gold province, southeast Australia. *Australian Journal of Earth Sciences* **48**, 883–99

Bons, P. D., Arnold, J., Elburg, M. A., Kalda, J., Soesoo, A. & van Milligen, B. P. 2004. Melt extraction and accumulation from partially molten rocks. *Lithos* **78**, 25–42.

Bowen, N. L 1928. *The evolution of the igneous rocks.* Princeton University Press.

Cashman, K. & Blundy, J. D. 2000. Degassing and crystallisation of ascending andesite and dacite. *Philosophical Transactions of the Royal Society of London* **A358**, 1487–513.

Castro, A., Patiño Douce, A. E., Corretge, L. G., de la Rosa, J., El-Biad, M. & El Hmidi, H. 1999. Origin of peraluminous granites and granodiorites, Iberian massif, Spain: an experimental test of granite petrogenesis. *Contributions to Mineralogy and Petrology* **135**, 255–76.

Chappell, B. W., White, A. J. R. & Wyborn, D. 1987. The importance of residual source material (restite) in granite petrogenesis. *Journal of Petrology* **28**, 1111–38.

Chappell, B. W., White, A. J. R. & Williams, I. S. 1991. A Transverse Section Through Granites of the Lachlan Fold Belt. *Second Hutton Symposium Excursion Guide*. Canberra: Bureau of Mineral Resources.

Chappell, B. W., White, A. J .R. & Wyborn, D. 1993. The Cowra Granodiorite and its enclaves. *Excursion guide, IAVCEI Canberra, Canberra*, Australian Geological Survey Organisation Record **67.**

Chappell, B. W. & Stephens, W. E. 1988. Origin of infracrustal (I-type) granite magmas. *Transactions of the Royal Society of Edinburgh: Earth Sciences* **79**, 71–86.

Chappell, B. W. & White, A. J. R. 1974. Two contrasting granite types. *Pacific Geology* **8**, 173–4.

Chappell, B. W. & White, A. J. R. 1992. I- and S-type granites in the Lachlan Fold Belt. *Transactions of the Royal Society of Edinburgh: Earth Sciences* **83**, 1–26.

Chen, Y. & Williams, I. S. 1990. Zircon inheritance in mafic inclusions from Bega Batholith granites, southeastern Australia: An ion microprobe study. *Journal of Geophysical Research* **95**, 17787–96.

Cherniak, D. J., Hanchar, J. M. & Watson, E. B. 1999. Diffusion of tetravalent cations in zircon. *Contributions to Mineralogy and Petrology* **127**, 383–90.

Clemens, J. D. 1989. The importance of residual source material (restite) in granite petrogenesis: a comment. *Journal of Petrology* **30**, 1313–16.

Clemens, J. D. 2003. S-type granitic magmas-petrogenetic issues, models and evidence. *Earth Science Reviews* **61**, 1–18.

Clemens, J. D. & Wall, V. W. 1981. Origin and crystallisation of some peraluminous (S-type) magmas. *Canadian Mineralogist* **19**, 111–31.

Clemens, J. D. & Wall, V. W. 1984. Origin and evolution of a peraluminous ignimbrite suite: the Violet Town Volcanics. *Contributions to Mineralogy and Petrology* **88**, 354–71.

Collins, W. J. 1996. Lachlan Fold Belt granitoids: products of three component mixing. *Transactions of the Royal Society of Edinburgh: Earth Sciences* **88**, 171–81.

Collins, W. J. 1998. Evaluation of petrogenetic models for Lachlan Fold Belt granitoids: implications for crustal architecture and tectonic models. *Australian Journal of Earth Sciences* **45**, 483–500.

Corfu, F., Hanchar, J. M., Hoskin, P. W. O. & Kinny, P. 2003. Atlas of zircon textures. *In* Hanchar, J. M. & Hoskin, P. W. O. (eds) *Zircon. Reviews in Mineralogy and Geochemistry* **53**, 468–500.

Couch, S., Sparks, R. S. J. & Carroll, M. R. 2001. Mineral disequilibrium in lava explained by convective self-mixing in open magma chambers. *Nature* **411**, 1037–9.

Davidson, J. P., Hora, J. M. Garrison, J. M. & Dungan, M. A 2005. Crustal forensics in arc magmas. *Journal of Volcanology and Geothermal Research* **140**, 157–70.

Davidson, J. P. 2007. *Transactions of the Royal Society of Edinburgh: Earth Sciences* **97** (for 2006), 000–000.

DePaolo, D. J. 1981. Trace element and isotopic effects of combined wallrock assimilation and fractional crystallisation. *Earth and Planetary Science Letters* **53**, 189–202.

Di Vincenzo, G., Andriessen, P. A. M. & Ghezzo, C. 1996. Evidence of two different components in a Hercynian peraluminous cordierite-bearing granite: the San Basilio intrusion (central Sardinia, Italy). *Journal of Petrology* **37**, 1175–206.

Elburg, M. A. 1996. Genetic significance of multiple enclave types in a peraluminous ignimbrite suite, Lachlan Fold Belt, Australia. *Journal of Petrology* **37**, 1385–408.

Elburg, M. A. & Nicholls, I. A. 1995. The origin of microgranitoid enclaves in the S-type Wilson's Promontory Batholith, Victoria: evidence for magma mingling. *Australian Journal of Earth Sciences* **42**, 423–35.

Glazner, A. F., Bartley, J. M., Coleman, D. S., Gray, W. & Taylor, Z. T. 2004. Are plutons assembled over millions of years by amalgamation from small magma chambers? *GSA Today* **14**, 4–11.

Gray, C. M. 1984. An isotopic mixing model for the origin of granitic rocks in southeastern Australia. *Earth and Planetary Science Letters* **70**, 47–60.

Gray, C. M. 1990. A strontium isotope traverse across the granitic rocks of southeastern Australia: Petrogenetic and tectonic implications. *Australian Journal of Earth Sciences* **37**, 331–49.

Gray, D. R. & Foster, D. A. 1997. Orogenic concepts – application and definition: Lachlan Fold Belt, eastern Australia. *American Journal of Science* **297**, 859–91.

Griffin, W. L., Wang, X., Jackson, S. E., Pearson, N. J., O'Reilly, S. Y., Xu, X. & Zhou, X. 2002. Zircon chemistry and magma mixing, SE China: *In-situ* analysis of Hf isotopes, Tonglu and Pingtan igneous complexes. *Lithos* **61**, 237–69.

Healy, B., Collins, W. J. & Richards, S. W. 2004. A hybrid origin for Lachlan S-type granites: the Murrumbidgee Batholith example. *Lithos* **78**, 197–216.

Hine, R., Williams, I. S., Chappell, B. W. & White, A. J. R. 1978. Contrasts between I- and S-type granitoids of the Kosciuszko Batholith. *Journal of the Geological Society of Australia* **25**, 219–34.

Hoskin, P. W. O. 2000. Patterns of chaos: fractal statistics and the oscillatory chemistry of zircon. *Geochimica et Cosmochimica Acta* **64**, 1905–23.

Ireland, T. R., Flottmann, T., Fanning, C. M., Gibson, G. M. & Preiss, W. V. 1998. Development of the early Paleozoic Pacific margin of Gondwana from detrital-zircon ages across the Delamerian Orogen. *Geology* **26**, 243–6.

Keay, S., Collins, W. J. & McCulloch, M. T. 1997. A three component Sr–Nd isotopic mixing model for granitoid genesis, Lachlan Fold Belt, eastern Australia. *Geology* **25**, 307–10.

Kemp, A. I. S., Wormald, R. J., Whitehouse, M. J. & Price, R. C. 2005a. Hf isotopes in zircon reveal contrasting sources and crystallisation histories for alkaline to peralkaline granites of Temora, southeastern Australia. *Geology* **33**, 797–800.

Kemp, A. I. S., Whitehouse, M. J. Hawkesworth, C. J. & Alarcon, M. K. 2005b. The implications of zircon U–Pb isotope systematics for the genesis of metaluminous granites in the Lachlan Fold Belt, southeastern Australia. *Contributions to Mineralogy and Petrology* **150**, 230–49.

Kemp, A. I. S., Hawkesworth C. J., Paterson, B. A. & Kinny, P. 2006. Episodic growth of the Gondwana Supercontinent from hafnium and oxygen isotopes in zircon. *Nature* **439**, 580–3.

Kemp, A. I. S., Hawkesworth, C. J., Foster, G. L., Paterson, B. A., Woodhead, J. D., Hergt, J. M., Gray, C. M. & Whitehouse, M. 2007. Magmatic and crustal differentiation history of granitic rocks from Hf–O isotopes in zircon. *Science* **315**, 980–3.

Lackey, J. S., Valley, J. W. & Saleeby, J. B. 2005. Supracrustal input to magmas in the deep crust of Sierra Nevada batholith: evidence from high $\delta^{18}O$ zircon. *Earth and Planetary Science Letters* **235**, 315–30.

Langmuir, C. H. 1989. Geochemical consequences of *in situ* crystallisation. *Nature* **340**, 199–205.

Maas, R., Nicholls, I. A. & Legg, C. 1997. Igneous and metamorphic enclaves in the S-type Deddick Granodiorite, Lachlan Fold Belt, SE Australia: petrographic, geochemical and Nd–Sr isotopic evidence for crustal melting and magma mixing. *Journal of Petrology* **38**, 815–41.

McCulloch, M. T. & Chappell, B. W. 1982. Nd isotopic characteristics of S- and I-type granites. *Earth and Planetary Science Letters* **58**, 51–64.

McCulloch, M. T. & Woodhead, J. D. 1993. Lead isotopic evidence for deep crustal scale fluid transport during granite petrogenesis. *Geochimica et Cosmochimica Acta* **57**, 659–74.

O'Neil, J. R. & Chappell, B. W. 1977. Oxygen and hydrogen isotope relations in the Berridale Batholith. *Journal of the Geological Society, London* **133**, 559–71.

Peck, W. H., Valley, J. W. & Graham, C. M. 2003. Slow diffusion rates of O isotopes in igneous zircons from metamorphic rocks. *American Mineralogist* **88**, 1003–14.

Phillips, G. N., Wall, V. J. & Clemens, J. D. 1981. Petrology of the Strathbogie Batholith: a cordierite-bearing granite. *Canadian Mineralogist* **19**, 47–63.

Read, H. H. 1948. Granites and granites. *In* Gilluly, J. (ed.) *Origin of granite*. Geological Society of America Memoir **28**, 1–19.

Soesoo, A. 2000. Fractional crystallisation of mantle-derived melts as an alternative mechanism for some I-type granite petrogenesis: an example from the Lachlan Fold Belt, Australia. *Journal of the Geological Society, London* **57**, 135–49.

Thompson, A. B., Matile, L. & Ulmer, P. 2001. Some thermal constraints on crustal assimilation during fractionation of hydrous, mantle-derived magmas with examples from central Alpine batholiths. *Journal of Petrology* **43**, 403–22.

Valley, J. W. 2003. Oxygen isotopes in zircon. *In* Hanchar, J. M. & Hoskin, P. W. O. (eds) *Zircon. Reviews in Mineralogy and Geochemistry* **53**, 343–85.

Valley, J. W., Lackey, J. S., Cavosie, A. J., Clechenko, C. C., Spicuzza, M. J., Basei, M. A. S., Bindeman, I. N., Ferreira, V. P., Sial, A. N., King, E. M., Peck, W. H., Sinha, A. K. & Wei, C. S. 2005. 4.4 Billion years of crustal maturation: oxygen isotope ratios of magmatic zircon. *Contributions to Mineralogy and Petrology* **151**, 561–80.

Vasquez, J. R. & Reid, M. R. 2005. Probing the accumulation history of the voluminous Toba Tuff. *Science* **305**, 991–4.

Vernon, R. H. 1983. Restite, xenoliths and microgranitoid enclaves in granites. Journal and *Proceedings of the Royal Society of New South Wales* **116**, 77–103.

Vernon, R. H. 1991. Interpretation of microstructures of microgranitoid enclaves. *In* Didier, J. & Barbarin, B. (eds) *Enclaves and Granite Petrology*, 277–92. Amsterdam: Elsevier.

Vervoort, J. D., Patchett, P. J., Blichert-Toft, J. & Albarede, F. 1999. Relationships between Lu–Hf and Sm–Nd isotopic systems in the global sedimentary system. *Earth and Planetary Science Letters* **168**, 79–99.

Vielzeuf, D. & Montel, J. M. 1994. Partial melting of metagreywackes. Part 1. Fluid-absent experiments and phase relationships. *Contributions to Mineralogy and Petrology* **117**, 375–93.

Waight, T, E., Maas, R. & Nicholls, I. A. 2000. Fingerprinting feldspar phenocrysts using crystal isotopic composition stratigraphy: implications for crystal transfer and magma mingling in S-type granites. *Contributions to Mineralogy and Petrology* **139**, 227–39.

Waight, T. E., Maas, R. & Nicholls, I. A. 2001. Geochemical investigations of microgranitoid enclaves in the S-type Cowra Granodiorite, Lachlan Fold Belt, SE Australia. *Lithos* **56**, 156–86.

Watson, E. B. & Harrison, T. M. 2005. Zircon thermometer reveals minimum melting conditions on Earliest Earth. *Science* **308**, 841–4.

Weinberg, R. F. 2006. Melt segregation structures in granitic plutons. *Geology* **34**, 305–8.

Wiebe, R. A. & Collins, W. J. 1998. Depositional features and stratigraphic sections in granitic plutons: implications for the emplacement and crystallization of granitic magma. *Journal of Structural Geology* **20**, 1273–89.

Williams, I. S. 1992. Some observations on the use of zircon U–Pb geochronology in the study of granitic rocks. *Transactions of the Royal Society of Edinburgh: Earth Sciences* **83**, 447–58.

Woodhead, J. D. & Hergt, J. M. 2005. A preliminary appraisal of seven natural zircon reference materials for in situ Hf isotope determination. *Geostandards and Geoanalytical Research* **29**, 183 95.

Wyborn, D., Chappell, B. W. & Johnston, R. W. 1981. Three S-type volcanic suites from the Lachlan Fold Belt, southeast Australia. *Journal of Geophysical Research* **86**, 10335–48.

Wyborn, D. & Chappell, B. W. 1986. The petrogenetic significance of chemically-related plutonic and volcanic rock units. *Geological Magazine* **123**, 619–28.

Yang, J.-H., Wu, F.-Y., Chung, S. L., Wilde, S. A. & Chu, M. F. 2006. A hybrid origin for the Qianshan A-type granite, northeast China: geochemical and Sr–Nd–Hf isotopic evidence. *Lithos* **89**, 89–106.

A. I. S. KEMP[1], C. J. HAWKESWORTH, B. A. PATERSON and G. L. FOSTER, Department of Earth Sciences, University of Bristol, Bristol, BS8 1RJ UK.
[1]Present address: School of Earth Sciences, James Cook University, Townsville, Australia 4811
e-mail: tony.kemp@jcu.edu.au

P. D. KINNY, The Institute for Geoscience Research, Curtin University, Perth, Australia.

M. J. WHITEHOUSE, Swedish Museum of Natural History, Stockholm, Sweden.

R. MAAS, School Of Earth Sciences, University of Melbourne, Parkville, Victoria, Australia.

EIMF, Edinburgh Ion Microprobe Facility, School of Geosciences, University of Edinburgh, Edinburgh, UK.

MS received 4 May 2006. Accepted for publication 1 August 2007.